Experimental Measurements of Sonic Boom Signatures Using a Continuous Data Acquisition Technique

Floyd J. Wilcox, Jr., and Alaa A. Elmiligui
Langley Research Center, Hampton, Virginia

NASA STI Program . . . in Profile

Since its founding, NASA has been dedicated to the advancement of aeronautics and space science. The NASA scientific and technical information (STI) program plays a key part in helping NASA maintain this important role.

The NASA STI program operates under the auspices of the Agency Chief Information Officer. It collects, organizes, provides for archiving, and disseminates NASA's STI. The NASA STI program provides access to the NASA Aeronautics and Space Database and its public interface, the NASA Technical Report Server, thus providing one of the largest collections of aeronautical and space science STI in the world. Results are published in both non-NASA channels and by NASA in the NASA STI Report Series, which includes the following report types:

- TECHNICAL PUBLICATION. Reports of completed research or a major significant phase of research that present the results of NASA Programs and include extensive data or theoretical analysis. Includes compilations of significant scientific and technical data and information deemed to be of continuing reference value. NASA counterpart of peer-reviewed formal professional papers, but having less stringent limitations on manuscript length and extent of graphic presentations.

- TECHNICAL MEMORANDUM. Scientific and technical findings that are preliminary or of specialized interest, e.g., quick release reports, working papers, and bibliographies that contain minimal annotation. Does not contain extensive analysis.

- CONTRACTOR REPORT. Scientific and technical findings by NASA-sponsored contractors and grantees.

- CONFERENCE PUBLICATION. Collected papers from scientific and technical conferences, symposia, seminars, or other meetings sponsored or co-sponsored by NASA.

- SPECIAL PUBLICATION. Scientific, technical, or historical information from NASA programs, projects, and missions, often concerned with subjects having substantial public interest.

- TECHNICAL TRANSLATION. English-language translations of foreign scientific and technical material pertinent to NASA's mission.

Specialized services also include organizing and publishing research results, distributing specialized research announcements and feeds, providing information desk and personal search support, and enabling data exchange services.

For more information about the NASA STI program, see the following:

- Access the NASA STI program home page at *http://www.sti.nasa.gov*

- E-mail your question to help@sti.nasa.gov

- Fax your question to the NASA STI Information Desk at 443-757-5803

- Phone the NASA STI Information Desk at 443-757-5802

- Write to:
  STI Information Desk
  NASA Center for AeroSpace Information
  7115 Standard Drive
  Hanover, MD 21076-1320

Experimental Measurements of Sonic Boom Signatures Using a Continuous Data Acquistion Technique

Floyd J. Wilcox, Jr., and Alaa A. Elmiligui
Langley Research Center, Hampton, Virginia

Level of review: This material has been technically reviewed by a committee of peers.

Summary

A wind tunnel investigation was conducted in the Langley Unitary Plan Wind Tunnel (UPWT) to determine the effectiveness of a technique to measure aircraft sonic boom signatures using a single conical survey probe while continuously moving the model past the probe. Sonic boom signatures were obtained using both move-pause and continuous data acquisition methods for comparison. The test was conducted using an existing generic business jet model at a constant angle of attack and a single model-to-survey-probe separation distance. The sonic boom signatures were obtained at a Mach number of 2.0 and a free-stream unit Reynolds number of 2 million per foot. The test results showed that it is possible to obtain sonic boom signatures while continuously moving the model, and that the time required to acquire the signature is at least 10 times faster than the move-pause method.

Introduction

Experimental research to measure sonic boom signatures of aircraft in wind tunnels has been conducted since the 1950s using a variety of techniques (ref. 1–14). One common technique is to use slender conical pressure probes to measure the sonic boom pressure signature of the aircraft model (ref. 2–9). The basic test technique consists of mounting a reference probe and a survey probe to the tunnel sidewall. The reference probe is mounted so that it remains in the free-stream flow at all times during the test. The survey probe is located so that as the aircraft model is moved longitudinally in the tunnel, the pressure field generated by the aircraft passes over the survey probe. The pressure difference between the reference and survey probe is measured with a differential pressure transducer that is sized for the small pressure differences to be measured. A typical run begins with the model located so that the nose shock is downstream of the survey probe. The model is then moved forward in small increments and paused as each point in the sonic boom pressure signature is measured. The length of time required to measure the entire sonic boom signature is dependent on the model size and can be significant if the model is large or the number of data points acquired is large.

Another technique that has been employed to measure sonic boom pressure signatures is similar to the slender probe technique described above except that the survey probe is replaced with a flat plate that has static pressure orifices on the surface of the plate (ref. 1 and 2).

Recently, long rails with multiple static pressure orifices located along the surface have been used to measure sonic boom signatures (ref. 10–14). With this technique, the entire sonic boom pressure signature can be obtained in a single data point. Although this technique shows promise, it is still being developed.

One of the advantages of the slender conical probe technique is that multiple survey probes can be used concurrently to measure the sonic boom pressure signature directly under the aircraft model ("on track") and at locations to the side of the aircraft ("off track"). However, as mentioned previously, the time required to measure a complete sonic boom pressure signature can be significant, and, consequently, the testing costs can be considerable. The purpose of this investigation was to determine the effectiveness of a technique to measure sonic boom signatures using the slender conical probe technique while continuously moving the model past the probe rather than using a move-pause technique. The continuous data technique was expected to significantly reduce the time required to acquire an entire sonic boom pressure signature and, consequently, reduce wind tunnel testing costs.

In the present study, a wind tunnel test was conducted to measure the sonic boom pressure signature of an existing generic business jet model using a slender conical probe and acquiring

data using move-pause and continuous data acquisition techniques for comparison. The tests were conducted in the Langley Unitary Plan Wind Tunnel (UPWT) at a Mach number of 2.0 and a free-stream unit Reynolds number of 2 million per foot. The sonic boom signatures were obtained with the model at a single angle of attack ($\approx 2.3°$) and at a model nose to survey probe separation distance of 13.5 in.

Nomenclature

Abbreviations and Acronyms

AOA	angle of attack, deg
ID	inside diameter
NF	normal force, lbf
OD	outside diameter
PM	pitching moment, in·lbf
PRT	platinum resistance thermometer
psfa	pound-force per square foot absolute (lbf/ft^2)
psfd	pound-force per square foot differential (lbf/ft^2)
SLSLE	straight-line segmented leading edge
UPWT	Unitary Plan Wind Tunnel

Symbols

f_{avg}	number of continuous data frames averaged, frames
h	distance from model nose to survey probe measured perpendicular to tunnel sidewall (see figure 2b), in.
M	Mach number
p	free-stream static pressure, psfa
p_0	free-stream stagnation pressure, psfa
p_{ref}	reference probe pressure, psfa
q	free-stream dynamic pressure, psfa
Re	free-stream unit Reynolds number $\times 10^{-6}$, ft^{-1}
t_d	duration of a complete sonic boom pressure signature run, min.
T_0	free-stream stagnation temperature, °F
v	model longitudinal speed during continuous sweep runs, in/s
α	angle of attack, deg
$(\Delta p/p_{ref})_{avg}$	average sonic boom pressure signature parameter where $\Delta x \leq 21.25$ in.
$(\Delta p/p_{ref})_{cor}$	corrected sonic boom pressure signature parameter (see equation 1)
$(\Delta p/p_{ref})_{unc}$	uncorrected sonic boom pressure signature parameter
Δp	measured differential pressure between survey probe and reference probe, psfd
Δx	distance from model nose to survey probe orifices measured parallel to tunnel sidewall (see figure 2b), in.

Apparatus and Experimental Methods

Wind Tunnel Description

The wind tunnel test was conducted in the Langley Unitary Plan Wind Tunnel, which is a continuous flow, variable pressure supersonic wind tunnel. The tunnel contains two test sections that

are approximately 4 ft by 4 ft square and 7 ft long. Each test section covers only part of the Mach number range of the tunnel. The nozzle ahead of each test section consists of an asymmetric sliding block that allows continuous Mach number variation during tunnel operations from 1.5 to 2.9 in the low Mach number test section (#1) and 2.3 to 4.6 in the high Mach number test section (#2). A complete description of the facility along with test section calibration information is contained in reference 15.

The nominal free-stream conditions used during this investigation in test section #1 are shown in table 1. Test section #2 was not used for this investigation.

Table 1. Nominal free-stream test conditions

M	Re, ft^{-1}	p_0, psfa	T_0, °F	q, psfa	p, psfa
2.00	2.00	1253	125	448.5	160.2

The tunnel air dew point was maintained below -20°F (at atmospheric pressure) to minimize water vapor condensation effects.

General Test Description

Figure 1 shows a photograph and sketch of the wind tunnel test setup. One of the test section doors, which normally contains schlieren windows, was replaced with a solid steel door so that some of the sonic boom measurement hardware (free-stream reference probe, survey probe, and transducer box) could be attached to the tunnel sidewall. The reference probe was mounted to the tunnel sidewall above and slightly upstream of the survey probe using a fixed (non-movable) support bracket. The tip of the reference probe was located 10.00 in. from the tunnel sidewall. The survey probe was mounted to the sidewall near the tunnel centerline using a support that was part of a mechanism that could move the probe longitudinally in the test section. However, during this test the survey probe remained at a fixed longitudinal position for all runs. A transducer box was located above and downstream of the survey probe location and was used to house pressure transducers that measured the differential pressure between the reference and survey probes and a transducer that measured just the reference probe pressure. Figure 2 shows the relative positions of the sonic boom hardware. Figure 3 shows the overall dimensions of the reference probe mounting bracket, survey probe mechanism, and the transducer box. The Instrumentation and Measurements section gives details of the reference and survey probes.

The aircraft model used during this test had previously been tested in UPWT and was identified as the straight-line segmented leading edge (SLSLE) model. Figure 4 shows a sketch and photograph of the model. The SLSLE model was chosen for this test because it was available for the test and because data from a previous test were accessible for comparison. The SLSLE model was tested without boundary layer transition grit. The SLSLE configuration was designed using the following criteria:

- Cruise Mach number 2.00

- Beginning cruise weight .... 88,000 lbf

- Beginning cruise altitude .... 53,000 ft

- Sonic boom ground overpressure ....0.5 psfd

3

References 8 and 16 contain additional details about the overall design of the model.

The SLSLE model and sting were pinned together and were designed not to be taken apart. The sting was attached to the sonic boom angle of attack (AOA) mechanism, which was in turn attached to the tunnel roll coupling and model support system. The SLSLE model was tested with positive normal force in the horizontal plane, i.e., wings vertical for all of the sonic boom pressure signature runs.

The tunnel angle of attack mechanism was not used to set the model angle of attack and remained at a fixed position during this test. Instead, the sonic boom AOA mechanism was used to set the model angle of attack to approximately $2.3°$. The model angle of attack consisted of both the pitch angle set by the sonic boom AOA mechanism and deflection caused by aerodynamic loads. During this test, the AOA mechanism pitch angle was set to approximately $1.7°$ to match one of the settings used during the previous test of the SLSLE model in UPWT. Because data from a previous test that used the sonic boom AOA mechanism showed that the mechanism contained approximately $0.2°$ of play (movement of the pitch mechanism that was not indicated by a linear potentiometer located inside the mechanism), a jam nut was fabricated and installed in the mechanism to lock it at the required pitch angle. Figure 5 shows the jam nut installed in the sonic boom AOA mechanism.

The tunnel model support system was used to position the SLSLE model laterally and longitudinally in the test section relative to the survey probe. During this test, the model nose was positioned at $h \approx 13.5$ in. (see fig. 2b), then the tunnel model support system was disabled in the lateral direction to prevent h from varying during the test. The tunnel model support system longitudinal movement capability was used to move the SLSLE model past the survey probe so that the sonic boom signature could be measured. During each pressure signature run, the model was moved longitudinally approximately 16.5 in.

During a typical run, the SLSLE model was initially positioned so that the nose shock was located downstream of the survey probe. For the move-pause runs, the model was moved forward in 0.125 in. increments while the model sonic boom pressure signature data were acquired. For the continuous sweep runs, the model was again positioned so that the nose shock was located downstream of the survey probe. The data acquisition system was started, and approximately 10 s of data were acquired before the model movement began. After the model was moved forward the required distance, the model movement was stopped and data were acquired for an additional 10 s.

Instrumentation and Measurements

Shown in figure 6 are sketches of the survey and reference probes. The probes were identical $4°$ included angle cones with two orifices drilled through the probe and into a central chamber. For these tests, the reference probe orifices were oriented such that one orifice was on top of the probe and the other on the bottom of the probe when viewing the probe from the side, i.e., looking into the sidewall. The survey probe orifices should have been oriented the same as the reference probe; however, because of an installation mistake, they were oriented such that one orifice was facing the tunnel sidewall used to mount the probes, and the other was facing toward the model. Because all of the sonic boom pressure signature data were acquired with the survey probe in the same orientation, the installation mistake had no effect on the conclusions of this test. The lengths of stainless steel tubing used to connect the reference and survey probes to the pressure transducers located in the transducer box are noted in figure 6. The final pressure connections inside the transducer box used flexible tubing (7/32 in. outside diameter, OD, by 3/32 in. inside diameter, ID).

Figure 7 shows a schematic of the reference and survey probe connections to the pressure

transducers. A solenoid activated valve that could be remotely operated was used to equalize the pressures across the differential pressure transducer to minimize the risk of over pressurizing the transducer during tunnel start and stops. The differential pressure between the reference and survey probes was measured with a ±13.006 psfd (±2.5 in. water column) pressure transducer, which had a quoted accuracy of ±0.018 psfd in the manufacturer's product literature. An in-situ calibration of the differential pressure transducer was performed, and the uncertainty in the difference between the applied and measured pressures, otherwise know as the regression uncertainty, was ±0.016 psfd at a 95 % confidence level. In addition, the reference probe pressure was measured directly with a 720 psfa absolute pressure transducer, which had a manufacturer's quoted accuracy of ±0.72 psfa. An in-situ calibration of the absolute pressure transducer was performed, and the regression uncertainty was ±0.172 psfa at a 95 % confidence level.

The transducer box was located on the tunnel sidewall above and downstream of the reference and survey probes. The purpose of the transducer box was to house the differential and absolute pressure transducers as close to the reference and survey probes as possible to minimize pressure lag effects. The transducer box was sealed, and the inside was maintained at near atmospheric conditions so that there would be no significant temperature or pressure effects on the pressure transducers. The solenoid activated valve was also located inside the transducer box. Figure 8 shows the inside of the transducer box with the two pressure transducers and solenoid valve. The transducer box was sized to house three differential pressure transducers so that in the future three survey probes could measure on-track and off-track pressure signatures concurrently.

The transducer box was fabricated out of aluminum with a polycarbonate insulating cover, which can be seen in figure 1a. The aluminum box was water cooled using 0.125 in. OD copper tubing epoxied into grooves machined into the sides, top, and bottom of the box. There were four separate cooling circuits for the left side, right side, top, and bottom of the transducer box. Cooling water was supplied to each circuit, and the water flow was controlled with a small brass needle valve. In addition to the water cooling, atmospheric air was circulated inside the box to help maintain a constant temperature inside the box. Two 0.5 in. OD nylon tubes were routed to the box and were used to supply cooling air to the box using a vacuum cleaner to pull atmospheric air through one of the nylon tubes into the box and then out the second nylon tube. Six type T (copper/copper-nickel) thermocouples were installed inside the transducer box to monitor the differential pressure transducer, air, and transducer box wall temperatures.

Force and moment data on the SLSLE model were measured with a 2-component electrical strain gage balance that was integral to the sting. The strain gages were located near the aft end of the sting and were covered with auto body filler that was faired to the sting contour. Two platinum resistance thermometers (PRT) were installed on the sting; one near the forward balance bridge and the second near the aft balance bridge. The purpose of the PRTs was to monitor the temperature gradient across the balance bridges and not to compensate for balance sensitivity changes caused by temperature. Figure 9 shows the locations of the model and balance moment reference centers. The full scale balance limits are shown in table 2.

Table 2. Range of balance components

Balance component	Range
normal force	±5 lbf
pitching moment	±109.2 in·lbf

The tunnel stagnation pressure was measured with a 100 psia bourdon tube pressure transducer that had a manufacturer's quoted accuracy of ±0.003 psia at a 95 % confidence level. The tunnel stagnation temperature was measured with a PRT.

The model support system lateral and longitudinal movement were measured by rotary encoders. The estimated accuracy of the model support system position based on calibration data was ±0.005 in. for both the longitudinal and lateral positions.

The model support system angle of attack was measured with an accelerometer mounted to the support system just downstream of the roll coupling. The model support system angle of attack was adjusted so that the sonic boom angle of attack mechanism was level before the SLSLE model was rolled to the wings vertical position. The tunnel model support angle of attack mechanism was not adjusted after leveling the sonic boom angle of attack mechanism.

The sonic boom angle of attack mechanism pitch angle was measured with a linear potentiometer. As discussed earlier, a jam nut was used to lock the mechanism to a single pitch angle. However, the jam nut could have locked in some unknown pitch error caused by the sonic boom AOA mechanism play. Based on unpublished checks conducted during a previous test, the mechanism play (and, consequently, the unknown pitch error) was as large as $0.2°$. Because the sonic boom AOA reading probably contained some fixed unknown error, the computed SLSLE model nose separation distance, h, which was a function of the pitch angle, also probably contained some error. However, since the pitch angle was fixed for the entire test, the small error in h would be constant for the entire test and, therefore, would not affect the results or conclusions of the test.

Data were acquired in either a move-pause or continuous mode depending on the run. The data acquisition system scan rate for the move-pause runs was 30 frames/s for two seconds; all of the data acquired during the two second period were averaged. The data acquisition system scan rate for the continuous runs varied from 60 frames/s to 480 frames/s. The data acquisition system had a low pass filter (2-pole Butterworth) that was set to 1 Hz for most runs with a few runs set at 1000 Hz to determine the effect of filter setting on the continuous data acquisition.

Corrections

The data acquired during the test were not corrected for tunnel flow angularity. The model angle of attack and the position of the model nose relative to the conical survey probe were corrected for sting deflections caused by aerodynamic loads. Because the sonic boom angle of attack mechanism was locked at one position, the SLSLE model angle of attack remained at approximately $2.3°$ for the entire test.

Because of static pressure variation within the tunnel test section, when the reference and survey probes were in the free-stream flow, the measured differential pressure between the probes, Δp, was not equal to zero. Consequently, the uncorrected sonic boom pressure signature parameter, $(\Delta p/p_{ref})_{unc}$, was also not equal to zero when the model nose shock was located downstream of the survey probe. Therefore, the sonic boom pressure signatures were adjusted by averaging all $(\Delta p/p_{ref})_{unc}$ values with $\Delta x \leq 21.25$ in. during a signature run (survey and reference probes in the free-stream flow) and subtracting the average value from each $(\Delta p/p_{ref})_{unc}$ value, i.e.,

$$\left(\frac{\Delta p}{p_{ref}}\right)_{cor} = \left(\frac{\Delta p}{p_{ref}}\right)_{unc} - \left(\frac{\Delta p}{p_{ref}}\right)_{avg} \tag{1}$$

Figure 10 shows the corrected and uncorrected sonic boom pressure signatures as a function of Δx for a single run to illustrate the approximate magnitude of the correction. No additional corrections or adjustments were performed to the sonic boom pressure signature data. Globally,

the variation of $(\Delta p/p_{ref})_{cor}$ within a sonic boom pressure signature was significantly less than the correction $(\Delta p/p_{ref})_{avg}$, which is typical for sonic boom testing in UPWT.

Results and Discussion

All of the plots in this section will show the corrected sonic boom pressure parameter $(\Delta p/p_{ref})_{cor}$ as a function of Δx. As mentioned previously, the SLSLE model angle of attack remained approximately 2.3° for the entire test.

Comparison Between Tests

The sonic boom pressure signatures obtained with the move/pause method are first compared to data obtained in a previous test using the same method. The purpose of this comparison is to show that the setup used in the current test was satisfactory. Figure 11 shows a comparison between the sonic boom pressure signature data as a function Δx for two sets of three back-to-back repeat runs obtained during the current test and data acquired during the previous test of this model as described in reference 8. The two sets of back-to-back repeat runs were obtained on two different days. In general, the results show reasonable agreement between the six repeat runs of the current test. Comparison with the previous test data shows a slight positive shift in Δx for the previous data. However, the magnitude and location of the signature peaks compare well between the tests indicating that nothing significant had changed between the tests, which gave confidence that the current test setup was satisfactory. The cause of the Δx shift between the two tests is unknown.

One significant difference between the tests is shown near $\Delta x = 33$ in. The previous test data show a negative peak as the flow expands aft of the model wing, whereas the data for the current test flattens and does not peak. The differential pressure transducer that measured Δp was overscaled in this region, and an internal mechanical stop inside the transducer prevented over pressurization of the transducer. Although most details of the previous and current test were identical, the reference and survey probes for the previous test were 2° included angle cones while the current test used probes with 4° included angles. The larger angles on the reference and survey probes resulted in a larger measured Δp that caused the differential pressure transducer diaphragm to hit the mechanical stop, resulting in a constant millivolt output from the transducer. Because the purpose of this test was to compare move-pause and continuous data acquisition techniques, the over pressurization of the differential pressure transducer in a small localized region of the pressure signature did not affect the overall conclusions of this test.

Determining Model Movement Speed for Continuous Sweep Runs

The first step in conducting this wind tunnel test was to determine a reasonable speed to move the model during the continuous sweep runs; however, optimizing the model movement speed was not attempted during this test. Figure 12 shows a comparison between the first three back-to-back repeat runs that were obtained in a move-pause mode of operation and the continuous data at five longitudinal speeds that covered the range of speeds available. The speeds were set in the tunnel model control system as a percentage of the maximum speed available, as shown table 3. The continuous data were acquired in order from the fastest to the slowest speeds. The move-pause and continuous data shown in figure 12 were acquired on the same day.

Figure 12a shows the results for the fastest longitudinal speed ($v = 0.329$ in/s). Overall, the continuous data follows the move-pause data, and the magnitude of the signature peaks match the move-pause data. However, there is a slight shift in the entire signature in the increasing Δx

Table 3. Model longitudinal speed settings

Percentage	v, in/s
100	0.329
50	0.170
25	0.088
12.5	0.048
6.25	0.025

direction that is caused by pressure lag in the tubing between the reference and survey probes and the differential pressure transducer. The data also show slightly more unsteadiness compared to the move-pause data, which is expected because each move-pause data point was an average of 60 frames of data while the continuous data were not averaged. Figures 12b–12e show the results as the longitudinal speed is decreased. As the model longitudinal speed decreases, the shift in the continuous data in the increasing Δx direction is eliminated, and the continuous data essentially fall on top of the move-pause data. With decreasing model longitudinal speed, the unsteadiness of the continuous data basically forms a band that covers the move-pause data.

Based on the data in figure 12, it was decided to acquire the remaining continuous sweep data at a longitudinal speed of 0.088 in/s for comparison with the move-pause data. The decision was a compromise between how well the continuous data compared to the move-pause data and the duration of the continuous data sweep (t_d in the plot key). Optimization of the time required for a continuous data sweep was not considered during this test.

Move-pause and Continuous Data Repeatability

Figure 13 shows a comparison between two sets of three back-to-back repeat move-pause runs and three back-to-back continuous sweep runs that were acquired on two separate days. In general, these data indicate that the continuous data acquisition method does follow the trends and match the peaks of the move-pause sonic boom signatures while significantly reducing the time required to acquire a signature. The continuous sweep data does show more unsteadiness than the move-pause data because the continuous data are not averaged.

The extent of the continuous data unsteadiness is shown in figure 14, which shows three back-to-back move-pause repeat runs and two sets of continuous data acquired over approximately 30 seconds at $\Delta x = 23$ in. and 29 in. while the model was stationary ($v = 0$ in/s). These data show that the range of the sonic boom pressure signature parameter for the continuous data was approximately 0.005. Figure 15 shows histograms for the two continuous runs presented in figure 14. The histograms provide an overall view of the distribution of continuous data and an indication of the central tendency and scatter of the data. These two plots indicate that the continuous data obtained at a single Δx location is roughly normally distributed with no significant skewing as expected. The standard deviation of the data for $\Delta x = 23$ in. and $\Delta x = 29$ in. is 0.00075 and 0.00098, respectively.

Differential Pressure Transducer Variation

Because of the unsteadiness of the continuous data shown in figure 13, data were acquired to determine if the differential pressure transducer caused any of the unsteadiness. Figure 16 shows the variation of the reference and survey probe differential pressure transducer at a typical wind-on condition and a wind-off condition as a function of elapsed time. These continuous data were acquired with the model stationary ($v = 0$ in/s). The shape of the curves for $(\Delta p/p_{ref})_{unc}$ and Δp shown in figure 16a is essentially identical and illustrates that the unsteadiness of the sonic boom pressure parameter obtained during wind-on continuous data acquisition is primarily caused by the unsteadiness in the measured Δp value. The variation in p_{ref} has little effect on the on the overall shape of the $(\Delta p/p_{ref})_{unc}$ curve. The stepped appearance of p_{ref} is caused by the least significant bit fluctuations of the data acquisition system analog to digital converter. Figure 16b shows the variation of Δp and p_{ref} for a wind-off condition with the tunnel pressure at approximately 400 psfa. The steady decrease in p_{ref} is caused by the inability to perfectly balance the removal of air from the tunnel using vacuum pumps and the leaks in the tunnel circuit. The standard deviation of Δp with no flow is more than two orders of magnitude less than a typical wind-on condition as shown in table 4. These results indicate that the variation seen in $(\Delta p/p_{ref})_{unc}$ for wind-on continuous runs is primarily caused by the unsteadiness of the measured differential pressure rather than transducer unsteadiness.

Table 4. Differential pressure transducer standard deviation

Tunnel condition	Δp standard deviation
wind-on	0.1305 psfd
wind-off	0.0007 psfd

Smoothing Continuous Data

One method to reduce the unsteadiness of the continuous data is to perform a moving average on the data. Figure 17 shows comparisons between continuous data with and without applying a moving average. The number of data frames used in the moving averages varied from 61 to 481. The moving average was centered, i.e., for a given Δx value, the moving average with 61 frames of data was computed by averaging 61 frames of data beginning 30 frames before the given Δx value to 30 frames after the Δx value. The results show that as the number of frames used in the moving average increases, the data variation is reduced; however, the peaks in the sonic boom parameter distribution are also smoothed, thus reducing the magnitude of peaks. Therefore, a trade-off between smoothing the data and reducing the peaks must be considered. For this test, a moving average of 181 frames (fig. 17c) was chosen because it appeared to be the best compromise between smoothing the data and not significantly reducing the peaks. All of the moving average data shown in the remainder of this report use 181 frames of data for the moving average. Figure 18 compares the continuous data with a moving average applied with the move-pause data for both sets of three back-to-back repeat runs. Comparison between figure 18 and figure 13 show that the unsteadiness of the continuous data is significantly reduced by applying a moving average.

9

Comparison Between Move-pause and Continuous Data

Figure 19 shows the six repeat move-pause runs along with the mean of the six runs with confidence and prediction intervals at a 95 % confidence level. The appendix shows the equations used to compute the mean, confidence interval, and prediction interval. Because the Δx values measured in each run were different, the data were interpolated using a straight line fit between Δx values to obtain $(\Delta p/p_{ref})_{cor}$ values at consistent Δx values from 20 in. to 36 in. in steps of 0.125 in. These interpolated $(\Delta p/p_{ref})_{cor}$ values were then used to compute the mean, confidence intervals, and prediction intervals at each Δx.

Figure 20 shows the six repeat continuous data runs (no moving average applied) along with the mean of the six runs with confidence and prediction intervals at a 95 % significance level. The continuous data were interpolated with a straight line fit between the data points just as with the move-pause data to obtain $(\Delta p/p_{ref})_{cor}$ values at the same Δx locations as used with the move-pause runs. Finally, figure 21 shows the same continuous data results as figure 20 except that the continuous data has a moving average applied.

In general, the confidence intervals for the move-pause (fig. 19) and continuous data (moving average applied, fig. 21) are about the same magnitude as would be expected since the variation between each set of six repeat runs is about the same. These confidence intervals are generally smaller than the intervals for the continuous data (no moving average applied, fig. 20). The smaller confidence intervals are a result of the smaller variation between the repeat runs of both the move-pause and continuous data (moving average applied) compared to the variation between the repeat runs for the continuous data (no moving average applied). The results for the prediction intervals are similar.

Figure 22 shows a comparison between the mean values of the move-pause data and the continuous data with and without a moving average applied. The confidence interval on each set of mean values at a 95 % significance level are also shown. At the bottom of the figure is the difference between the means of the move-pause and continuous data along with the confidence interval at a 95 % significance level. The confidence interval on the difference in means was determined using a pooled variance because an F-distribution test (ref. 17) showed that the variation from the two sets of data were statistically equal.

Since the confidence interval on the difference in means in general encompasses 0 across the Δx range, there is no statistical difference between the move-pause data and the continuous data either with or without applying a moving average. The confidence interval on the difference in means is larger for the continuous data with no moving average applied than for the continuous data with a moving average applied, as would be expected. The confidence intervals for the difference in means where the nose shock begins (22.0 in. $\lesssim \Delta x \lesssim$ 22.5 in.) do not encompass 0 for the continuous data with a moving average applied; however, the difference in means at the peaks of the signatures shows no statistical difference across the entire signature. The difference in means plots indicate that the mean value of the sonic boom signature acquired by continuously moving the model is essentially equivalent to the mean value of a signature acquired with the move-pause technique. The real benefit to acquiring sonic boom signatures continuously is that the time required to acquire the signature is significantly less than for the move-pause technique as will be discussed in the next section.

Data Acquisition Time Savings

The key in figures 19 and 20 shows the duration required to acquire the entire sonic boom signature (t_d) for the move-pause and continuous data, respectively. The results show that a typical move-pause signature required approximately 52 minutes while the continuous data required ap-

proximately 3.5 minutes. The duration of the move-pause runs was longer than expected based on other sonic boom tests conducted previously in UPWT. The cause of the longer duration for the move-pause runs was a delay in the communication between the tunnel data acquisition system, which had just been replaced and was being used for the first time in a production wind tunnel test, and the tunnel model support control system. Because the duration of the move-pause runs was adversely affected by the communication delay, a direct comparison between the duration of the move-pause runs and the continuous runs was not attempted. Instead, the duration of move-pause runs for previous sonic boom tests conducted in UPWT was used in the comparison.

Previous sonic boom tests in UPWT typically acquired data using a move-pause technique with the distance between data points of 0.125 in., which is the same distance used in the current test. The time required to acquire sonic boom data points for these previous tests ranged from 14 s/pt to 24 s/pt. A 10 in. long signature would require 81 points and a duration of 18.9 min. to 32.4 min. as shown below:

14 (s/pt) (81 pt) = 1134 s = 18.9 min.

and

24 (s/pt) (81 pt) = 1944 s = 32.4 min.

During this test, the majority of continuous data were acquired at $v \approx 0.09$ in/s, which was a compromise between how well the continuous data compared to the move-pause data and the duration of the continuous data sweep. At this speed, a 10 in. long signature would require 1.85 min.

10 in. / (0.09 in/s) = 111.1 s = 1.85 min.

Therefore, the continuous data acquisition technique reduces the time required to acquire a sonic boom pressure signature by 10 to 17 times compared to the move-pause technique. Consequently, the total costs for a wind tunnel test would decrease because of the reduced tunnel occupancy costs and electrical energy costs.

Effect of Filter Setting

Figure 23 shows comparisons between the move-pause data and continuous data obtained at data acquisition low-pass filter setting of 1 Hz and 1000 Hz. The continuous data in these plots were acquired at the maximum longitudinal speed ($v = 0.329$ in/s) that the model support system could move the model. Typically, data in the UPWT are acquired with the data acquisition system filter set to 1 Hz. The results of these runs show that at a filter setting of 1 Hz, the continuous data are much smoother than the 1000 Hz data; however, at 1 Hz the data also show a slight time lag, i.e., Δx shift, compared to the move-pause data. The time lag is especially evident at the model nose shock (22.0 in. $\lesssim \Delta x \lesssim$ 22.5 in.).

As discussed earlier, optimization of the time required for a continuous data run was not considered during this test. However, the low-pass filter setting data suggest that it might be possible to adjust the data acquisition system filter setting and the model longitudinal speed setting to reduce the time required to obtain a complete sonic boom signature and still acquire data that compares favorably with the move-pause technique. The optimization of these factors would be a natural extension of this test.

Concluding Remarks

A wind tunnel investigation was conducted in the Langley Unitary Plan Wind Tunnel to determine the effectiveness of a technique to measure aircraft sonic boom signatures using a single conical survey probe while continuously moving the model past the probe. Sonic boom signatures were obtained using both move-pause and continuous data acquisition methods for comparison. The test was conducted using an existing generic business jet model at a constant angle of attack and a single model-to-survey-probe separation distance. The sonic boom signatures were obtained at a Mach number of 2.0 and a free-stream unit Reynolds number of 2 million per foot.

The following is a summary of the significant findings:

1. The means of the move-pause and continuous sonic boom pressure signature data were statistically equivalent.

2. Performing a moving average on the continuous data smoothed the data but did not significantly improve the comparison with the move-pause data.

3. The time required to measure a sonic boom signature using the continuous data technique was 10–17 times faster than the move-pause technique.

4. It might be possible to further decrease the time required to obtain a complete sonic boom signature using the continuous data technique by optimizing the model longitudinal speed, data acquisition rate, and data acquisition filter setting. Additional research would need to be conducted.

References

1. Carlson, Harry W.: *An Investigation of Some Aspects of the Sonic Boom by Means of Wind-Tunnel Measurements of Pressures about Several Bodies at a Mach Number of 2.01.* NASA TN D–161, 1959.

2. Carlson, Harry W.: *Correlation of Sonic-Boom Theory with Wind-Tunnel and Flight Measurements.* NASA TR R–213, 1964.

3. Mendoza, Joel P.; and Hicks, Raymond M.: *Further Studies of the Extrapolation of Near-Field Overpressure Data.* NASA TM X–2219, 1971.

4. Hunton, Lynn W.; Hicks, Raymond M.; and Mendoza, Joel P.: *Some Effects of Wing Planform on Sonic Boom.* NASA TN D–7160, 1973.

5. Carlson, H. W.; and Morris, O. A.: Wind-Tunnel Sonic-Boom Testing Techniques. AIAA Paper 66–765, 1966.

6. Carlson, Harry W.; Mack, Robert J.; and Morris, Odell A.: *A Wind-Tunnel Investigation of the Effect of Body Shape on Sonic-Boom Pressure Distributions.* NASA TN D–3106, 1965.

7. Carlson, Harry W.; and Mack, Robert J.: *A Study of the Sonic-Boom Characteristics of a Blunt Body at a Mach Number of 4.14.* NASA TP–1015, 1977.

8. Mack, Robert J.; and Kuhn, Neil: *Determination of Extrapolation Distance with Measured Pressure Signatures from Two Low-Boom Models.* NASA TM–2004–213264, 2004.

9. Wilcox, Floyd J., Jr.; Elmiligui, Alaa A.; Wayman, Thomas R.; Waithe, Kenrick A.; Howe, Donald C.; and Bangert, Linda S.: *Experimental Sonic Boom Measurements on a Mach 1.6 Cruise Low-Boom Configuration.* NASA TM–2012–217598, 2012.

10. Makino, Yoshikazu; Suzuki, Ken′ichiro; Noguchi, Masayoshi; and Yoshida, Kenji: Non-Axisymmetrical Fuselage Shape Modification for Drag Reduction of a Low Sonic-Boom Airplane. AIAA 2003–557, 2003.

11. Furukawa, Takeshi; Makino, Yoshikazu; Noguchi, Masayoshi; and Ito, Takeshi: Supporting System Study of Wind-Tunnel Models for Validation of Aft-Sonic-Boom Shaping Design. AIAA 2008–6596, 2008.

12. Durston, Donald A.; Cliff, Susan E.; Wayman, Thomas R.; Merret, Jason M.; Elmiligui, Alaa A.; and Bangert, Linda S.: Near-Field Sonic Boom Test on Two Low-Boom Configurations Using Multiple Measurement Techniques at NASA Ames. AIAA 2011–3333, 2011.

13. Cliff, S.; Elmiligui, A.; Aftosmis, M.; Thomas, S.; Morgenstern, J.; Durston, D.: Design and Evaluation of a Pressure Rail for Sonic Boom Measurements in Wind Tunnels. Seventh International Conference on Computational Fluid Dynamics, ICCFD7–2006, 2012.

14. Morgenstern, John M.: How to Accurately Measure Low Sonic Boom or Model Surface Pressures in Supersonic Wind Tunnels. AIAA 2012–3215, 2012.

15. Jackson, Charlie M., Jr.; Corlett, William A.; and Monta, William J.: *Description and Calibration of the Langley Unitary Plan Wind Tunnel.* NASA TP–1905, 1981.

16. Mack, Robert J.; and Kuhn, Neil S.: *Determination of Extrapolation Distance With Pressure Signatures Measured at Two to Twenty Span Lengths From Two Low-Boom Models.* NASA TM–2006–214524, 2006.

17. Montgomery, Douglas C.; and Runger, George C.: *Applied Statistics and Probability for Engineers.* Fifth ed., John Wiley & Sons, Inc. 2011.

Solid steel door blank

Reference probe

Transducer box

Survey probe mechanism

Survey probe

SLSLE model and sting

Instrumentation leads, cooling air, and cooling water

Model support system

Model support system AOA mechanism

Roll coupling

Sonic boom AOA mechanism

Flow

2012–L–03809
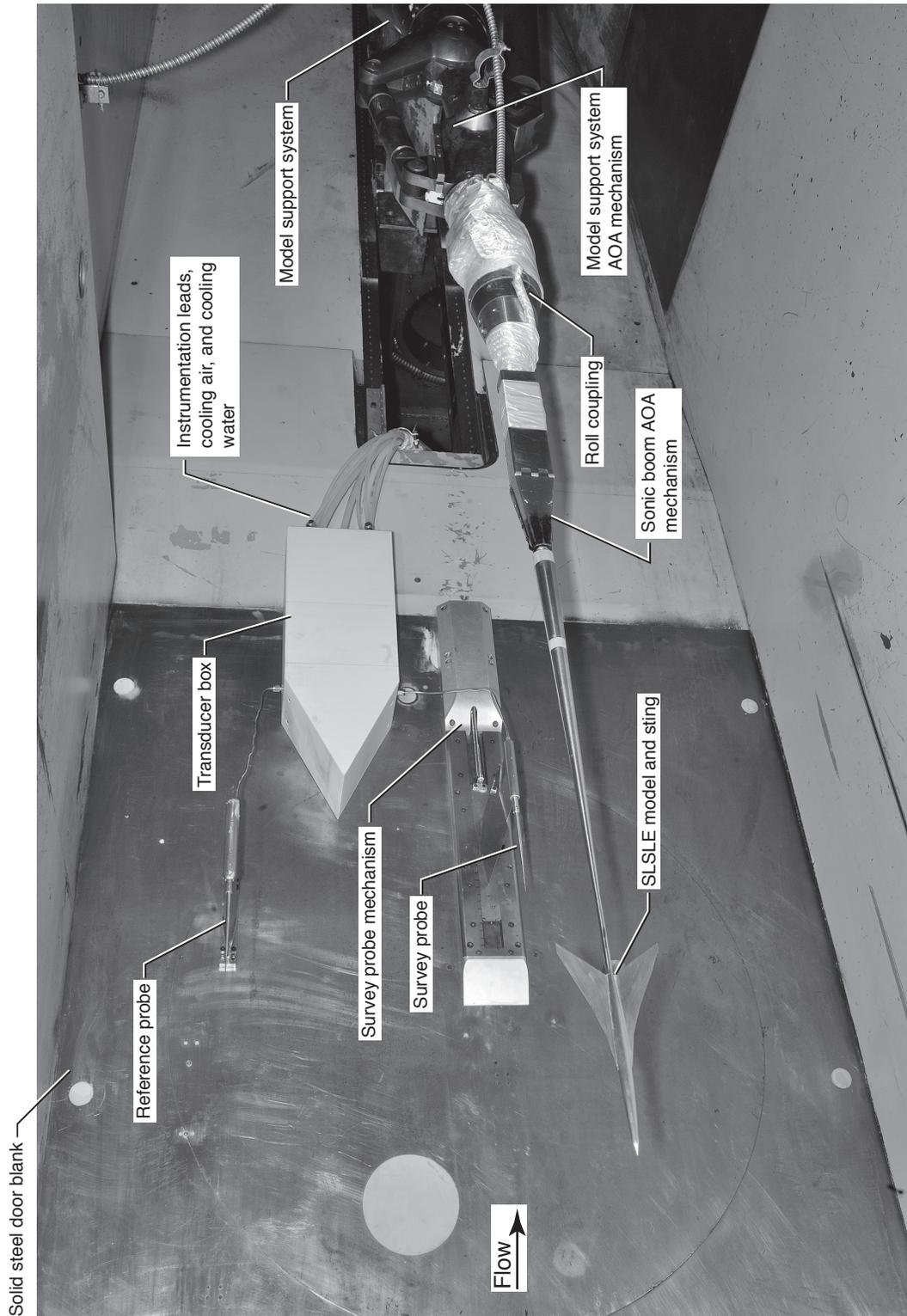
(a) Model mounted in wind tunnel.

Figure 1. General experimental test setup.

14
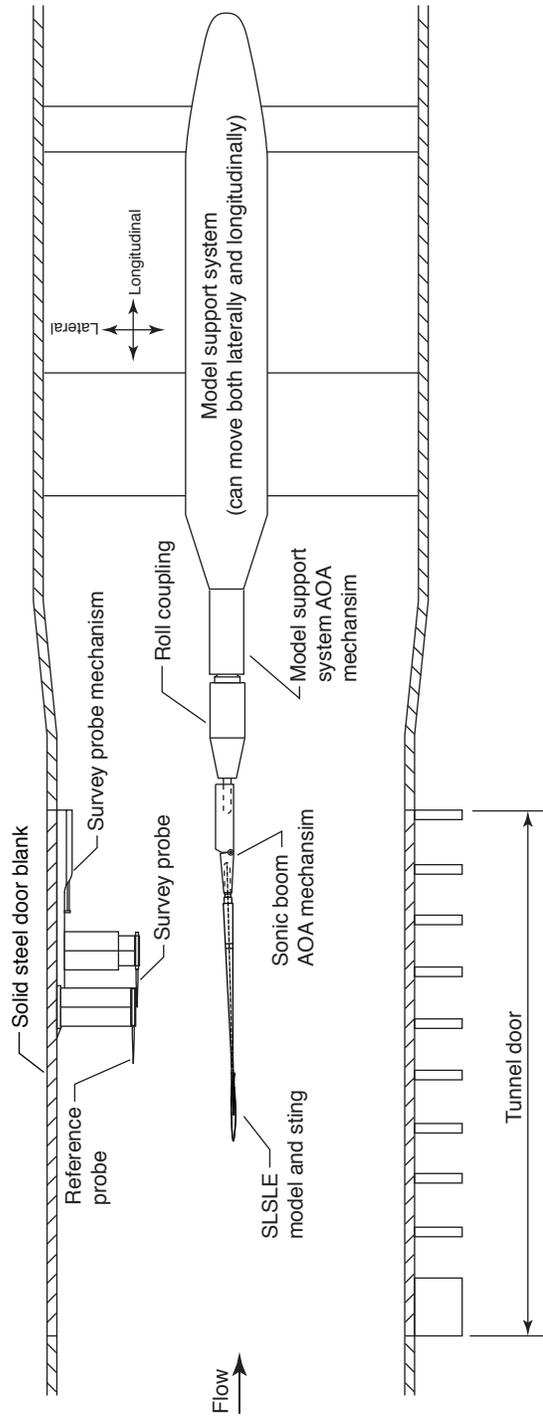
(b) Top view (transducer box removed for clarity).

Figure 1. Concluded.
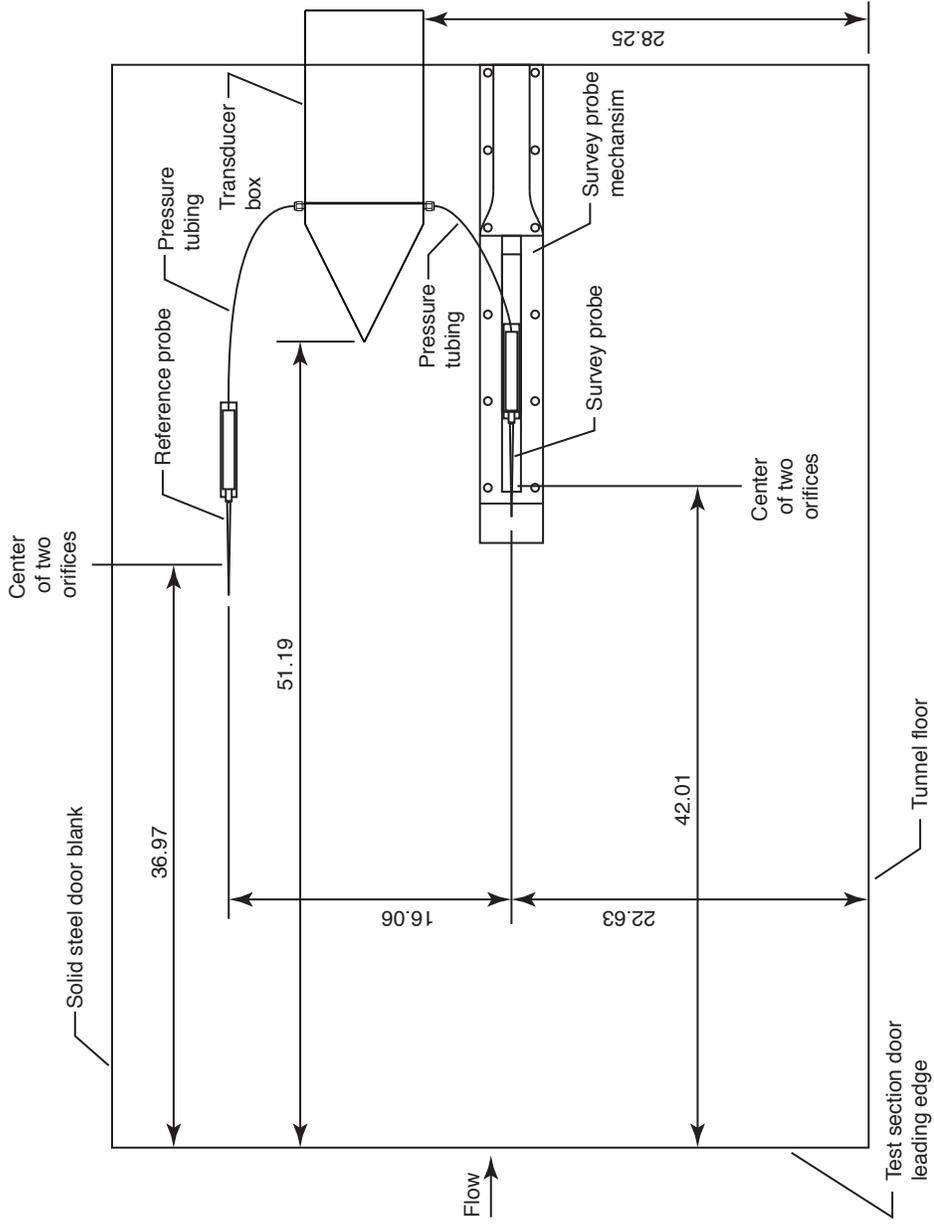
(a) Side view.

Figure 2. Details of the experimental setup. All dimensions are in inches.
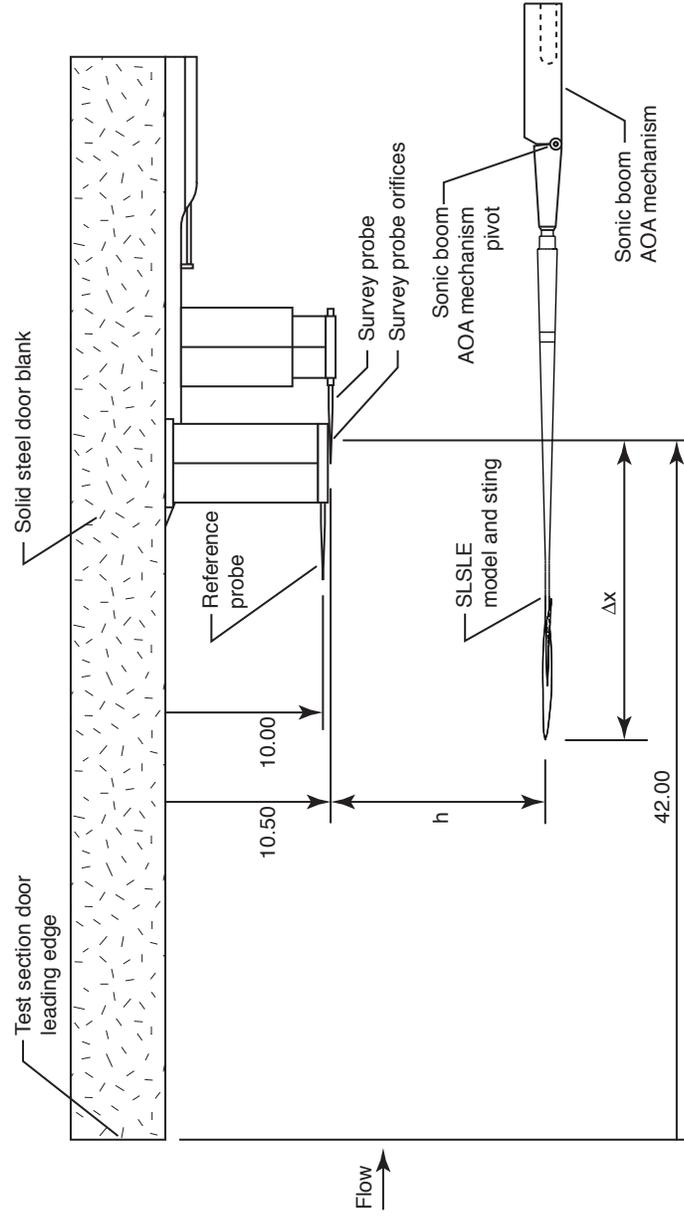
(b) Top view (transducer box removed for clarity).

Figure 2. Concluded.

17
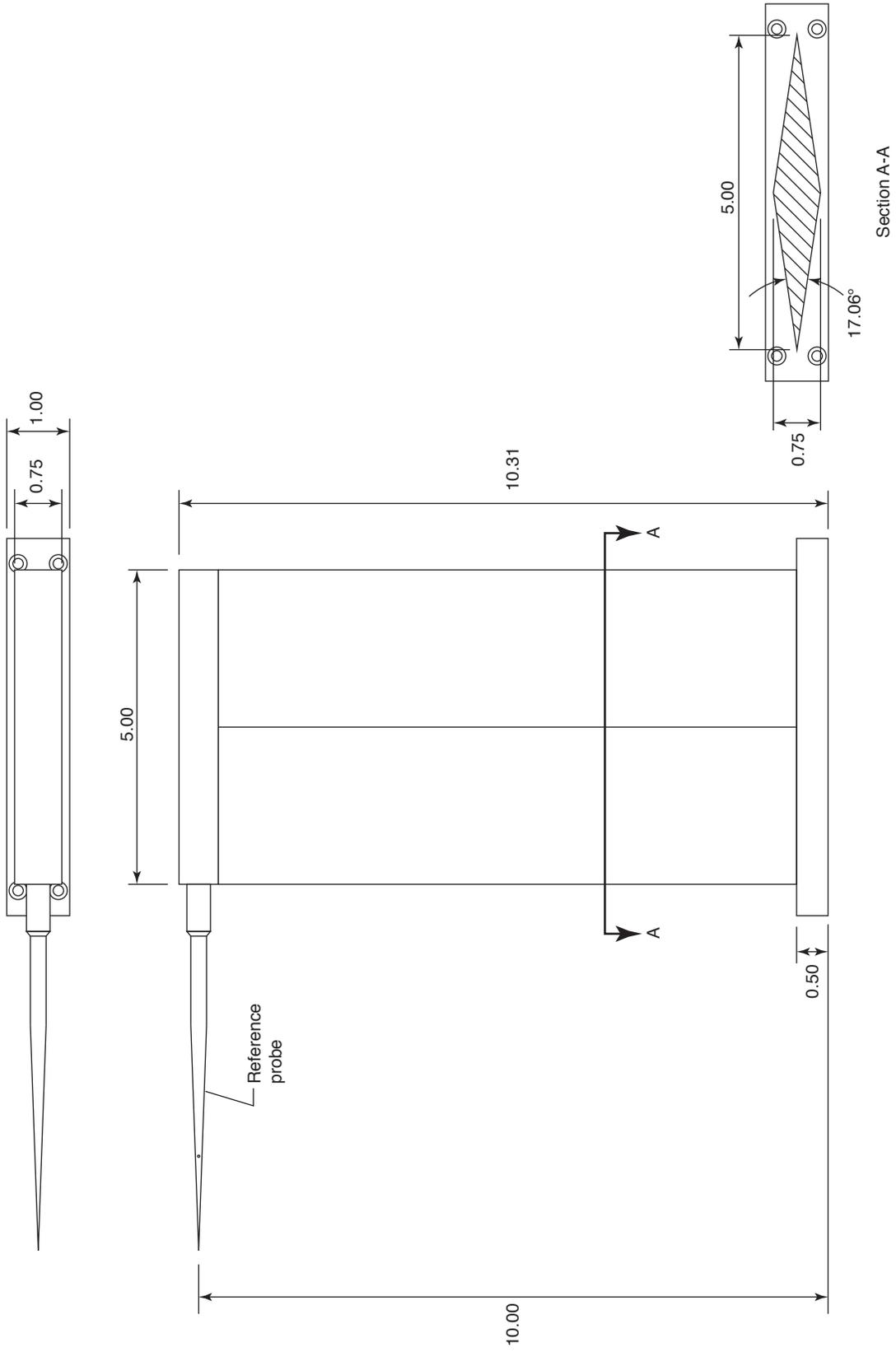
(a) Reference probe holder.

Figure 3. Various hardware sketches. All dimensions are in inches.
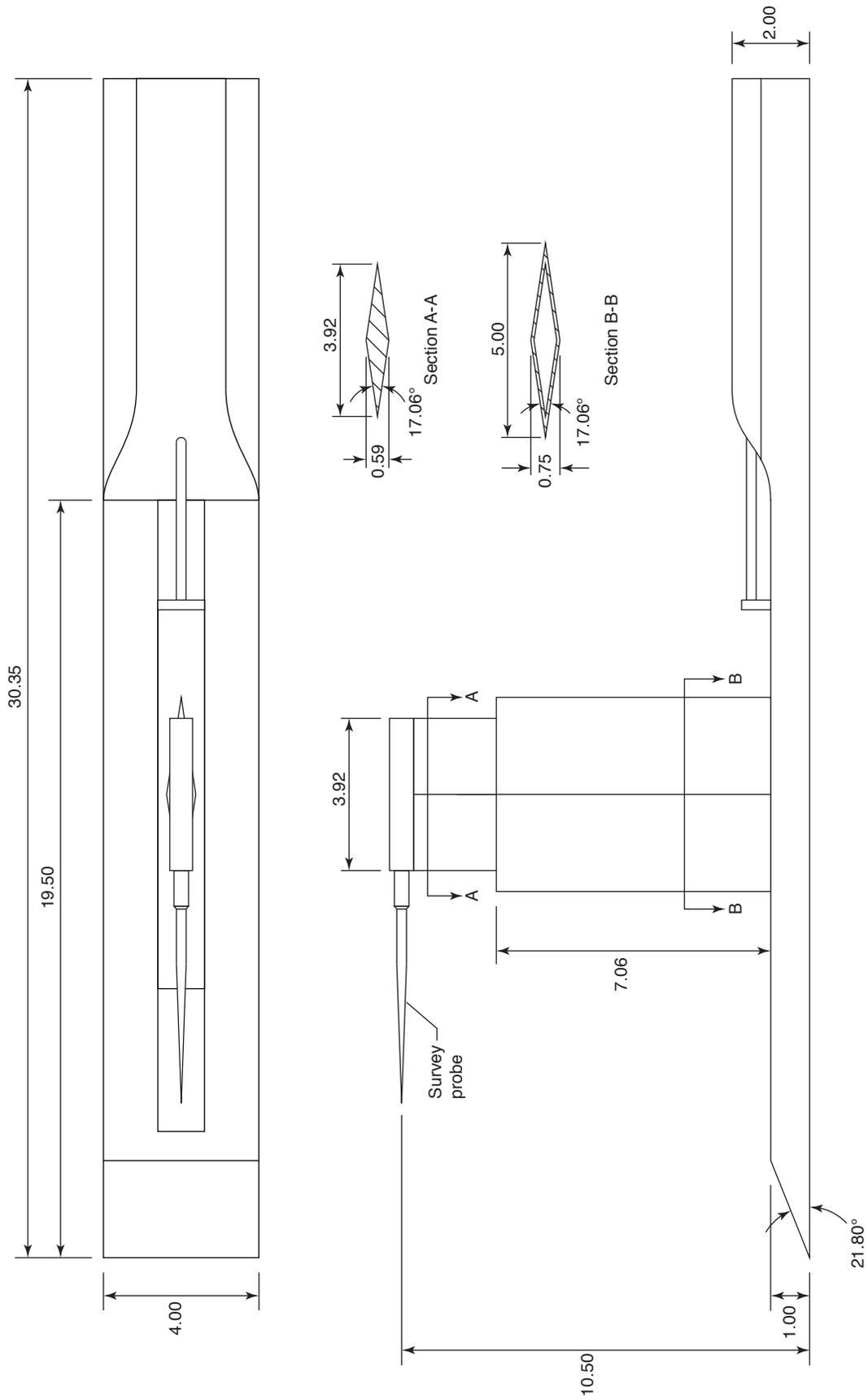
(b) Survey probe mechanism.

Figure 3. Continued.

Fitting for 0.125 dia. pressure tubing

53.1°

3.25

7.50

21.01

8.58

8.71

2.50

5.25
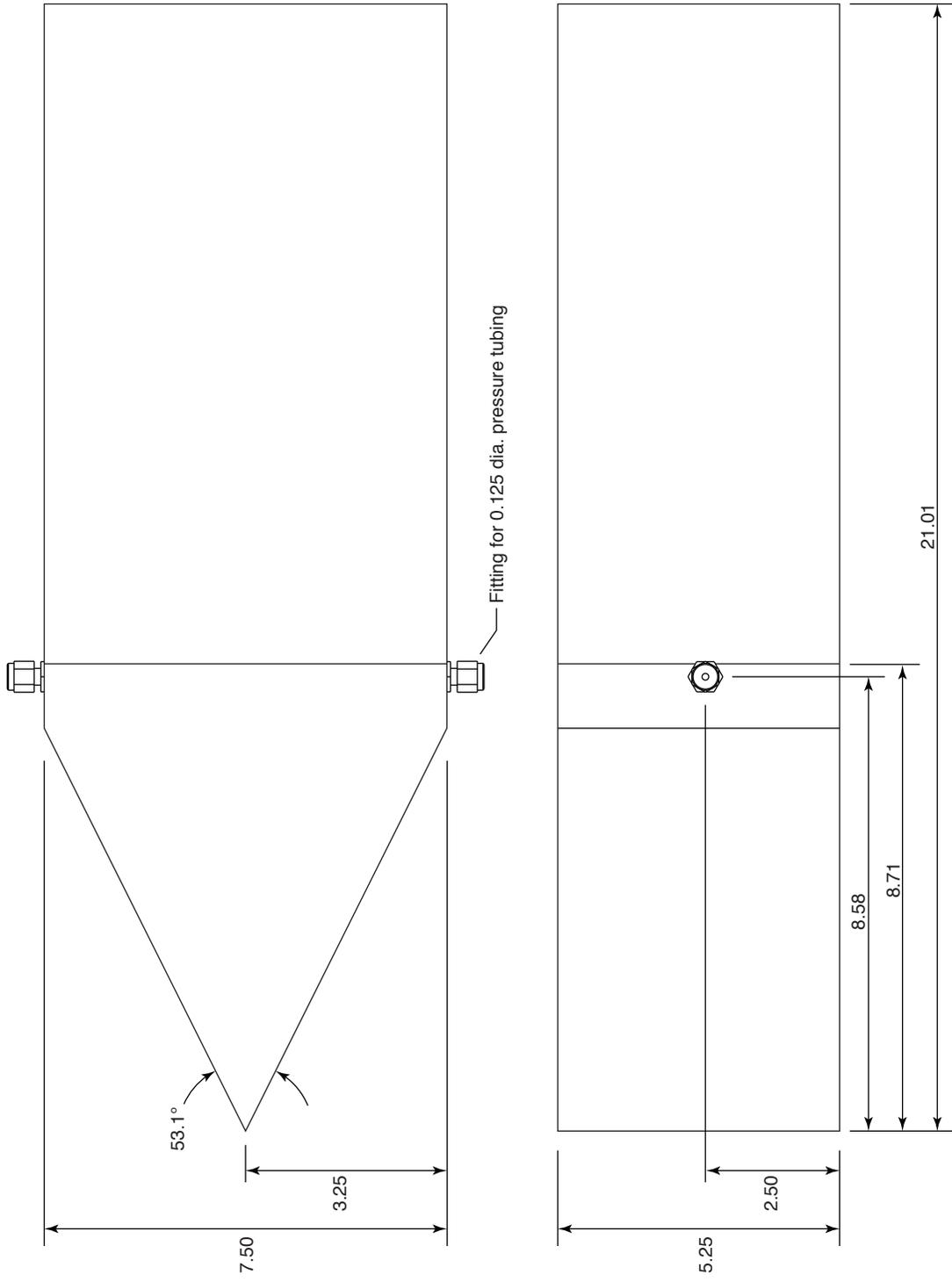
(c) Transducer box.

Figure 3. Concluded.

20
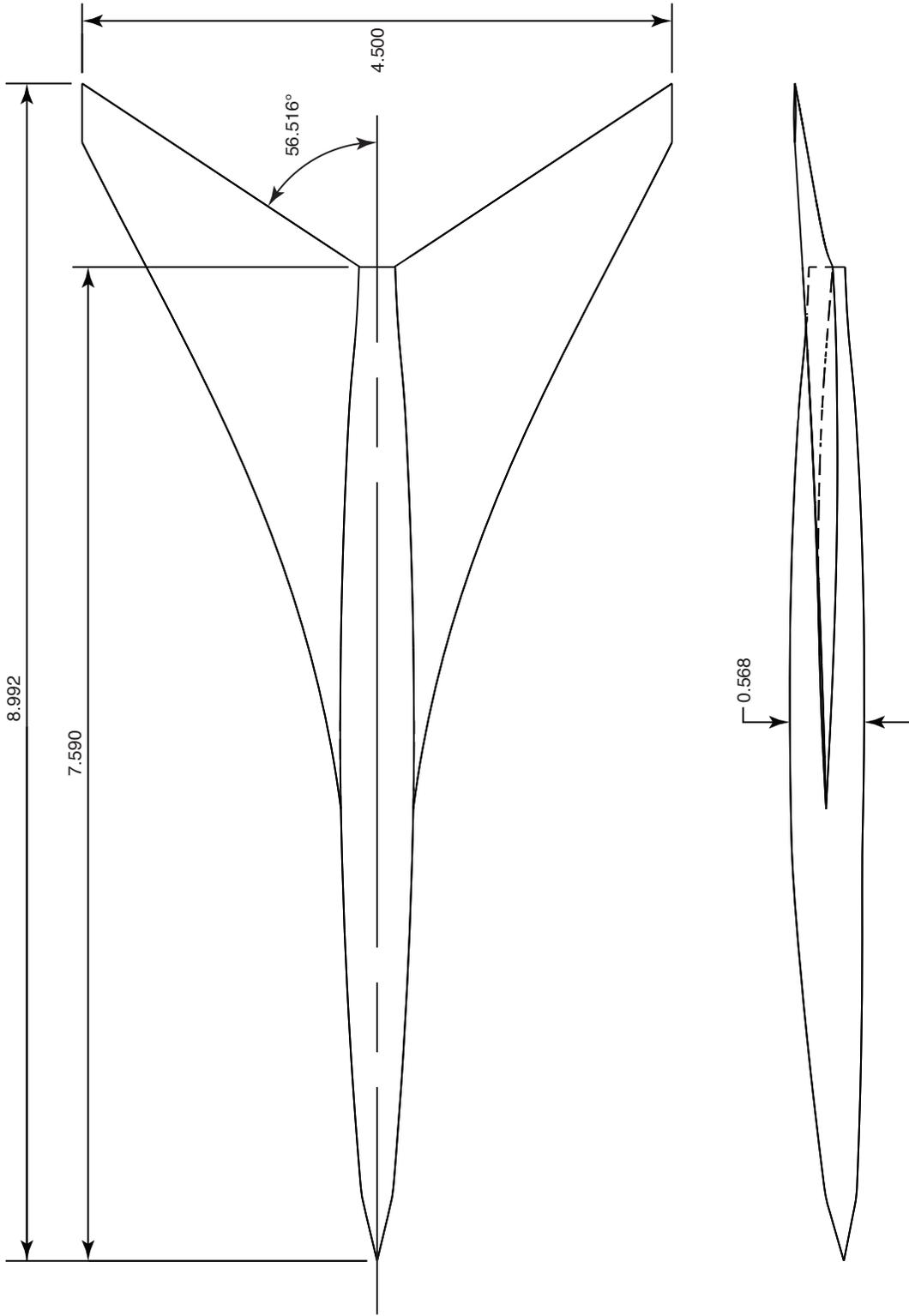
(a) Sketch with overall dimensions.

Figure 4. Straight-line segmented leading edge model description. All dimensions are in inches unless otherwise noted.

L-2003-01611

(b) Top view.

L-2003-01612

(c) Side view.

Figure 4. Concluded.
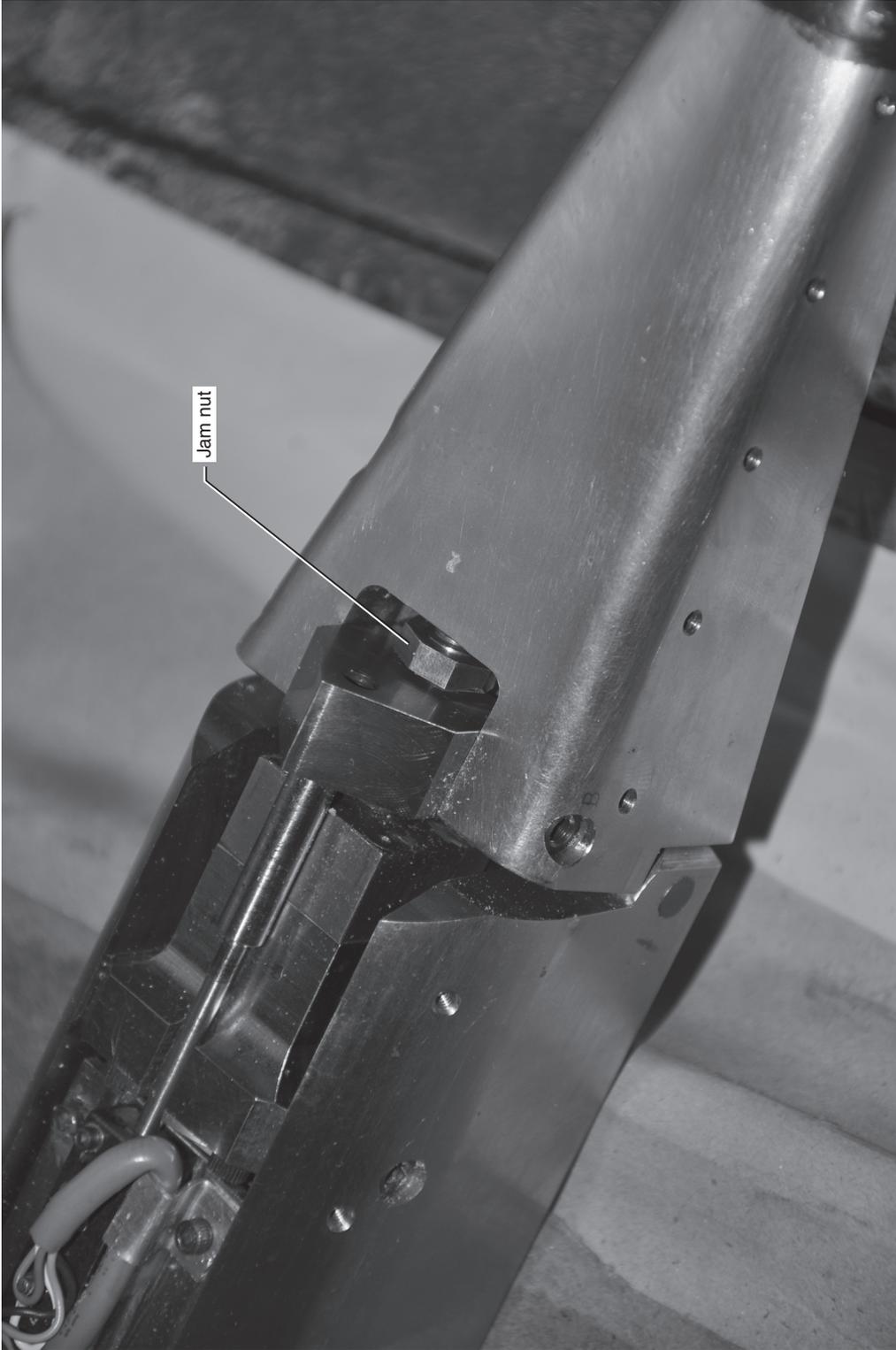
Jam nut

Figure 5. Jam nut used to lock the sonic boom angle of attack mechanism to one position.

0.375 dia.

0.188 dia.

Tubing,
0.125 dia. OD
0.070 dia. ID

A

9.925

0.075

0.250

5.000

3.580

0.035 dia. thru

4°

1.500

A

To pressure transducers

Tubing,
0.125 dia. OD
0.070 dia. ID

Tubing,
0.094 dia. OD
0.063 dia. ID

Section A-A
(sectioning excludes tubing)

0.050 dia.

Tubing lengths (approximate)

Probe	0.094 dia. OD	0.0125 dia. OD
Reference	15	7
Survey	3	19
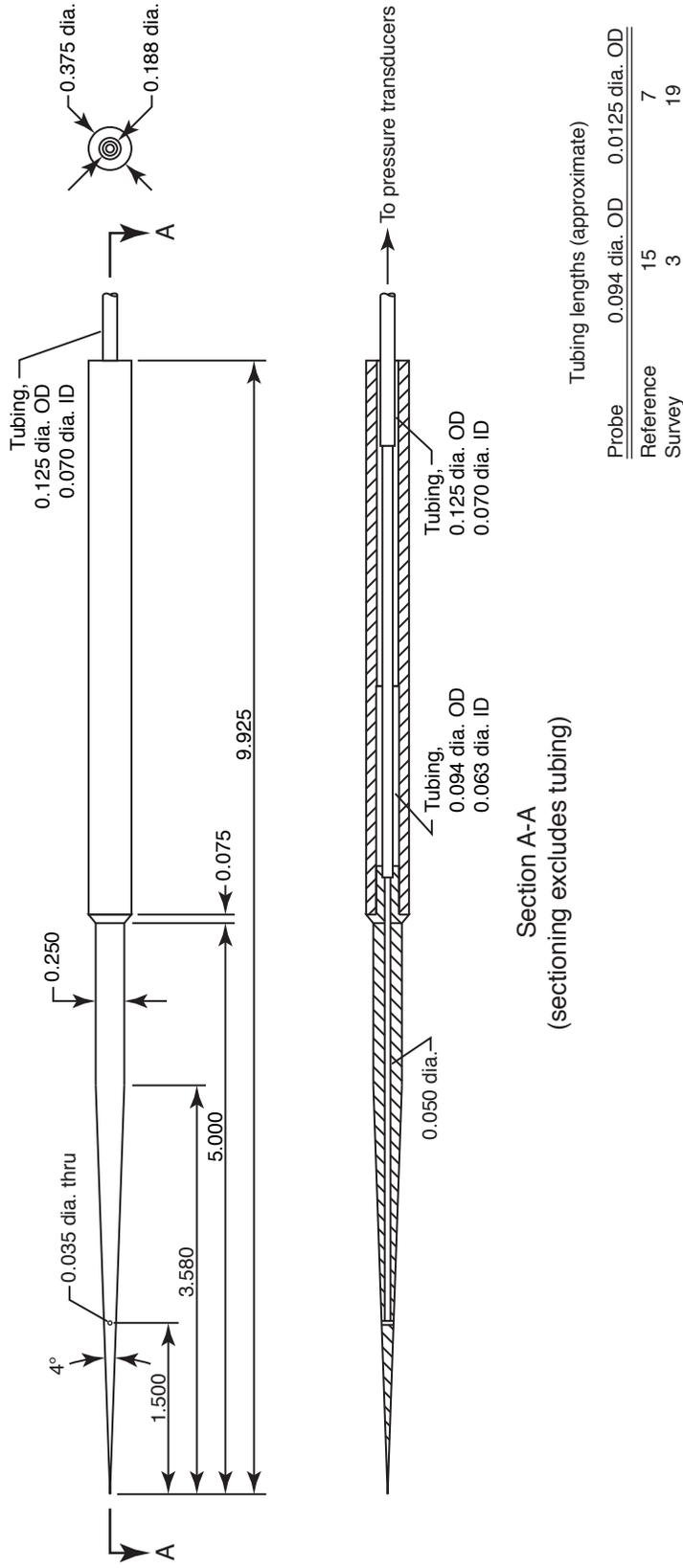
Figure 6. Reference and survey probe drawing. All dimensions are in inches unless otherwise noted.

24
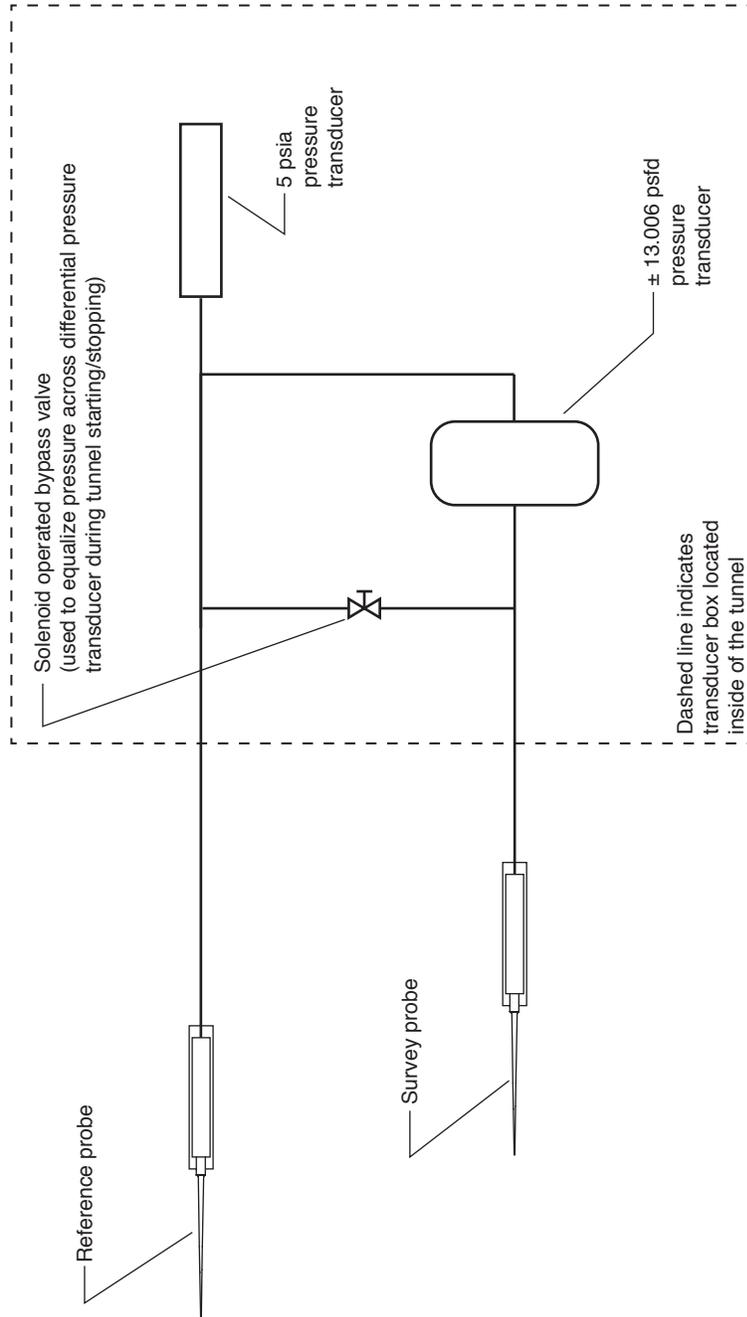
Figure 7. Reference and survey probe pressure hookup.

5 psia pressure transducer

± 13.006 psfd pressure transducer

Solenoid operated bypass valve (used to equalize pressure across differential pressure transducer during tunnel starting/stopping)

Dashed line indicates transducer box located inside of the tunnel

Reference probe

Survey probe

Cooling water

Instrumentation leads and cooling air

Solenoid bypass valve

5 psia pressure transducer

± 0.09 psid differential pressure transducer

2012–L–03808

Figure 8. Transducer box (insulating plastic cover removed).

26
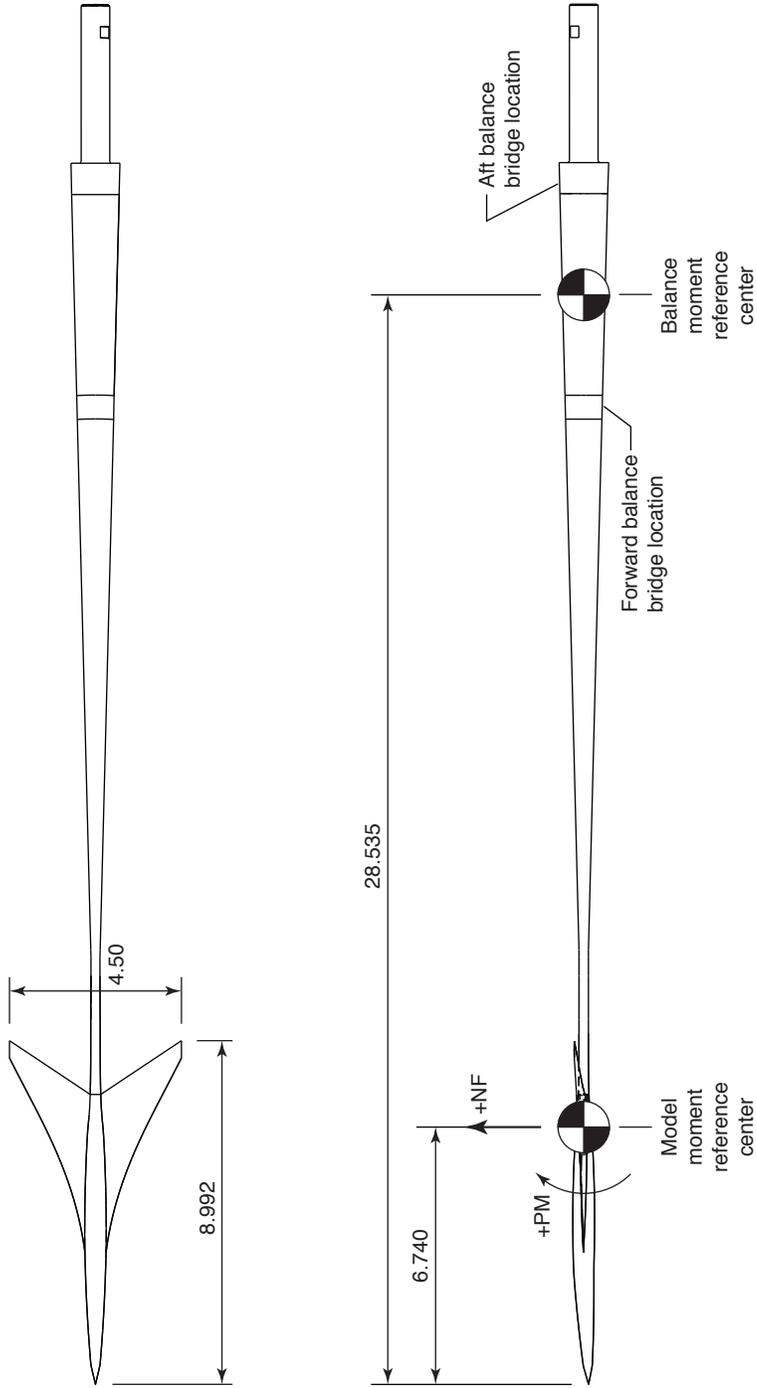
Figure 9. Moment reference center locations. All dimensions are in inches.
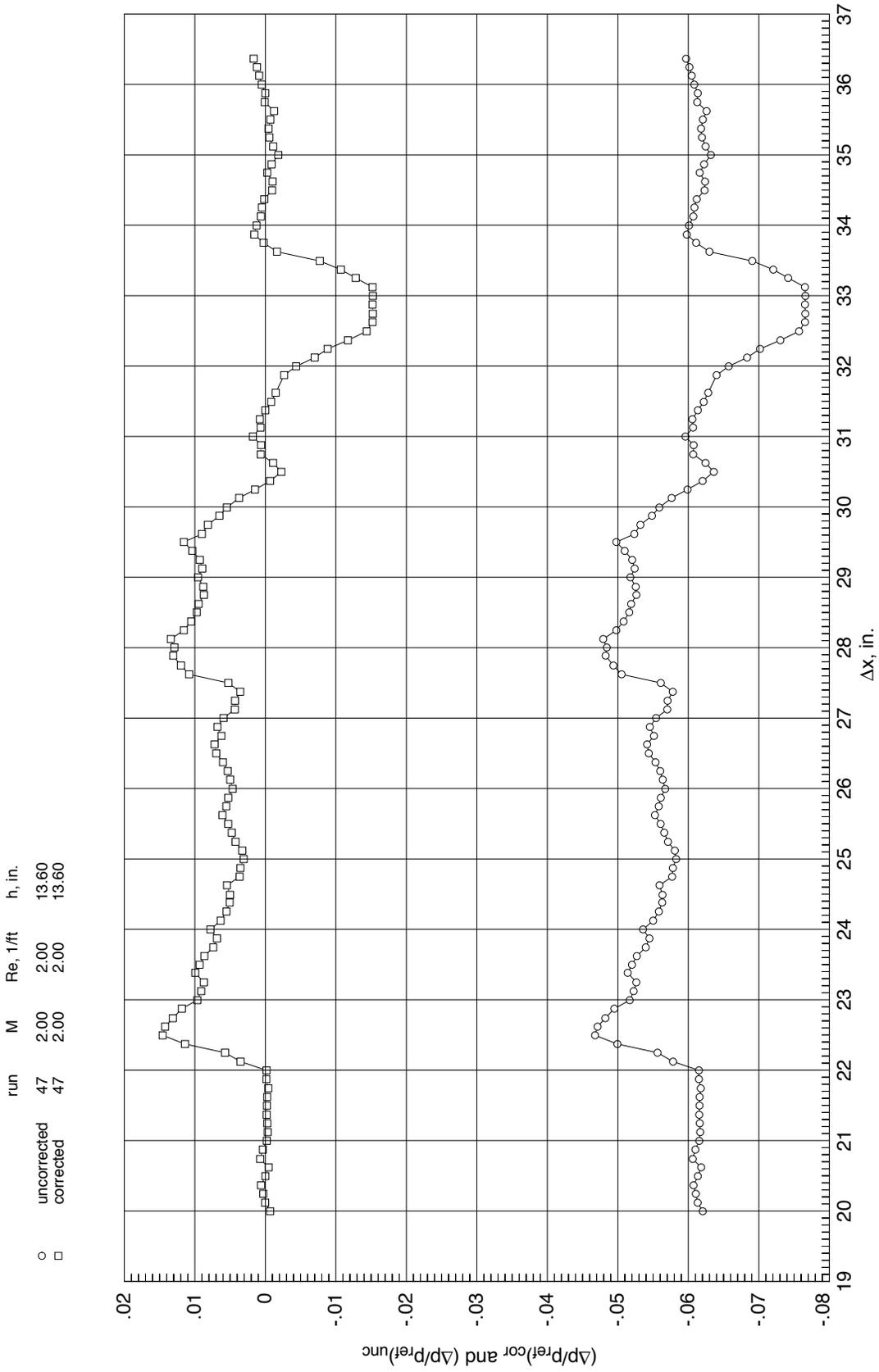
Figure 10. Comparison of uncorrected and corrected sonic boom pressure signatures.
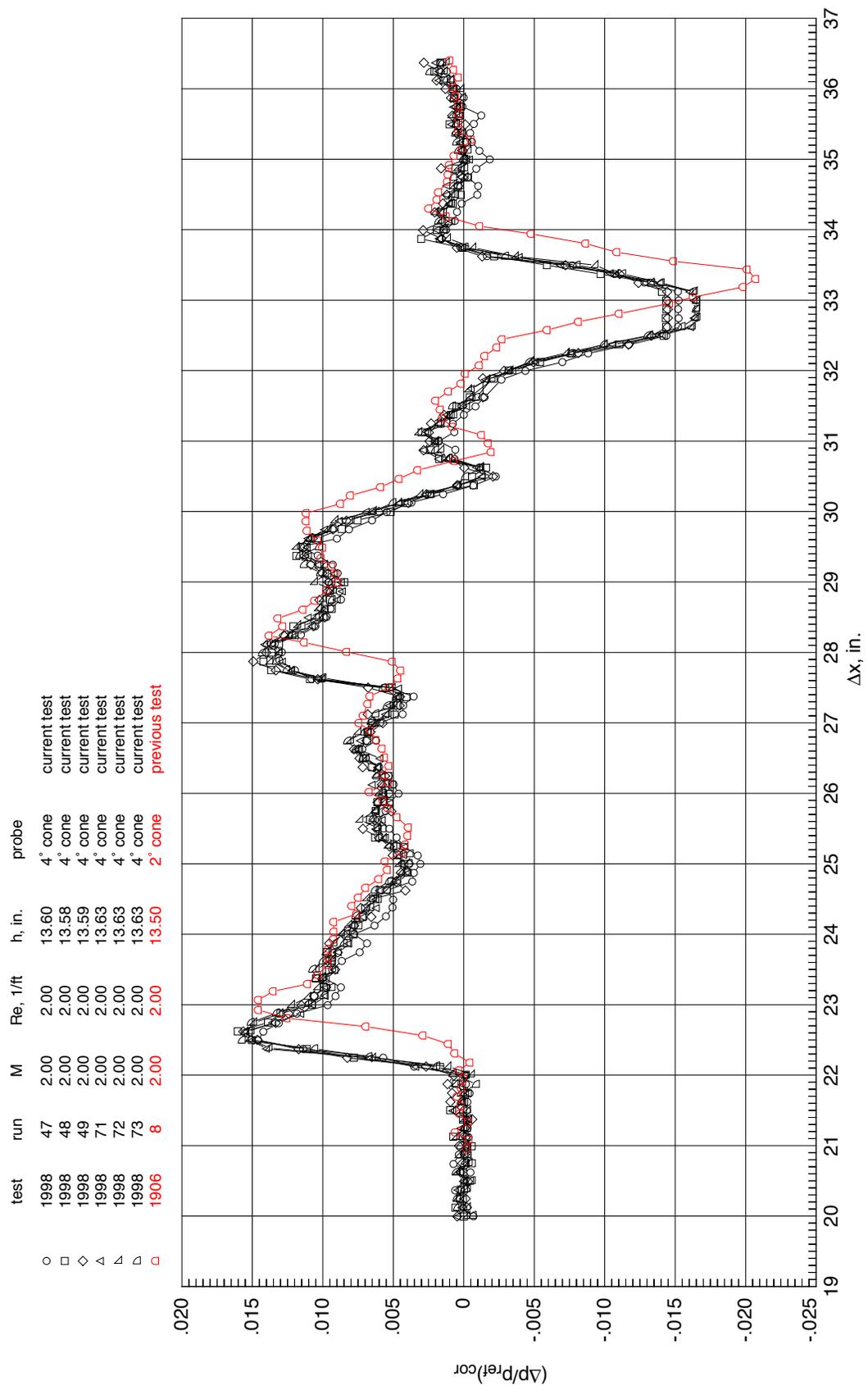
Figure 11. Sonic boom pressure signature comparison between tests.
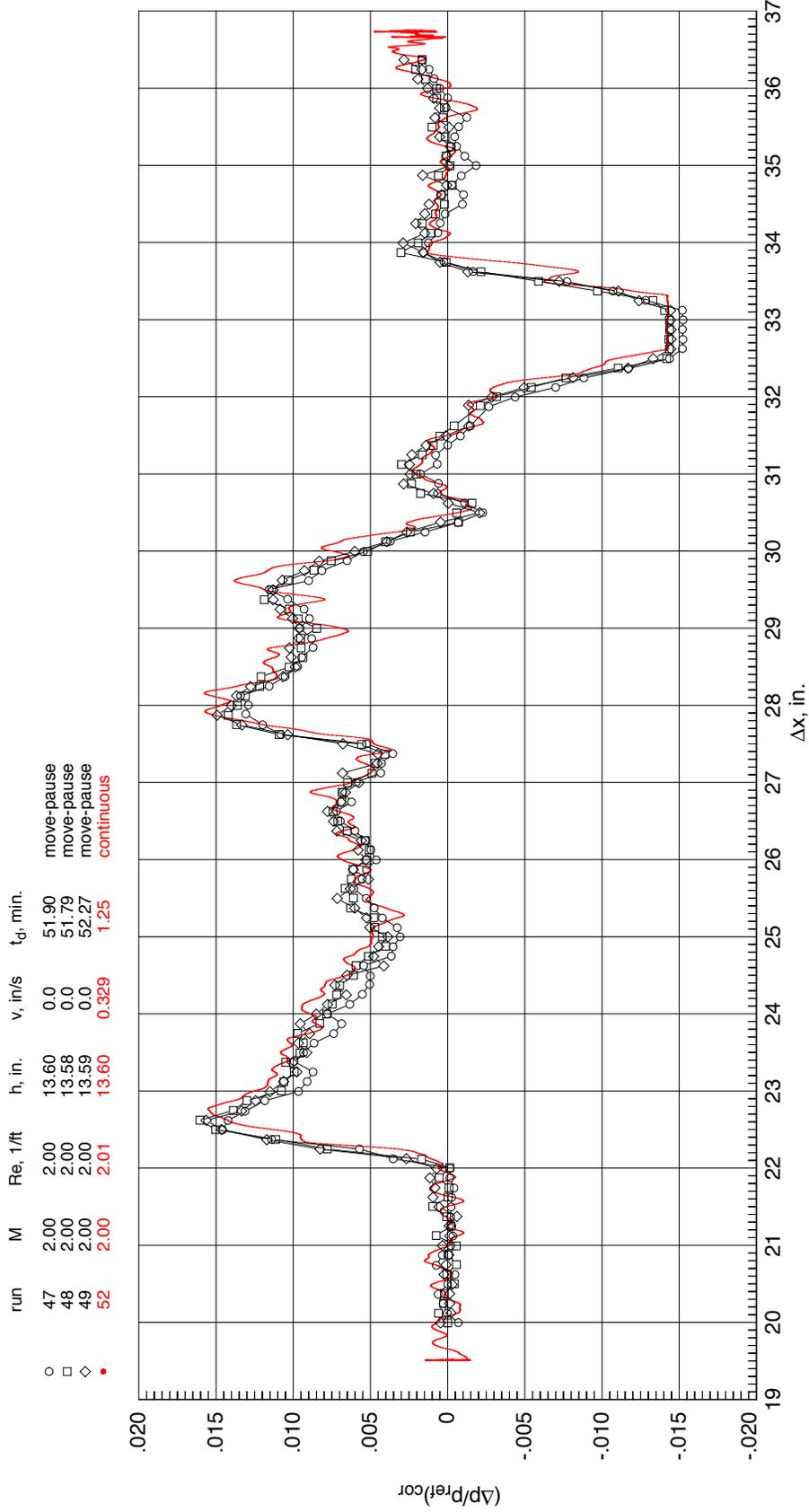
Figure 12. Comparison of sonic boom pressure signatures for move-pause and continuous data at various model longitudinal speeds.

(a) $v = 0.329$ in/s.
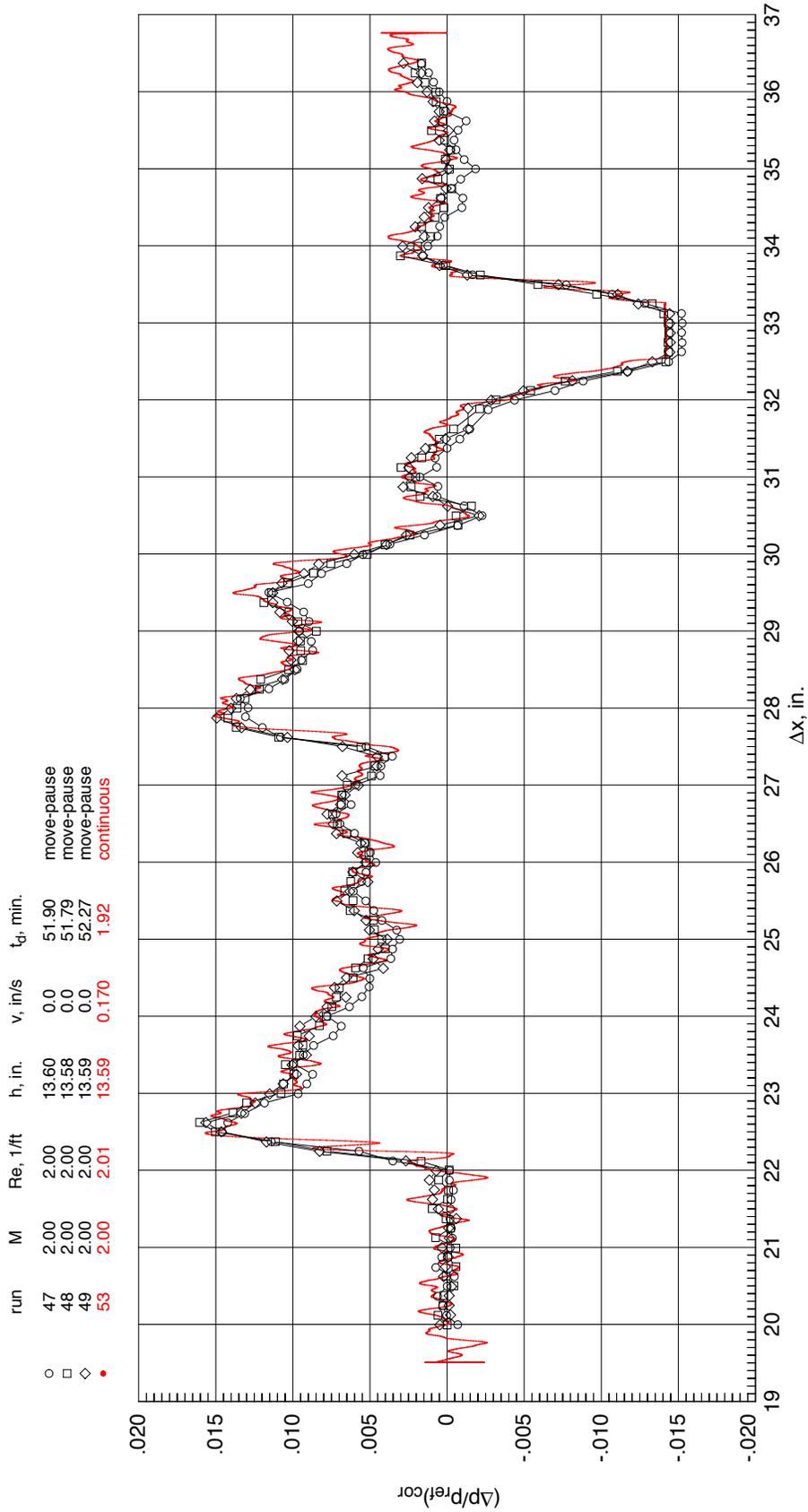
(b) $v = 0.170$ in/s.

Figure 12. Continued.
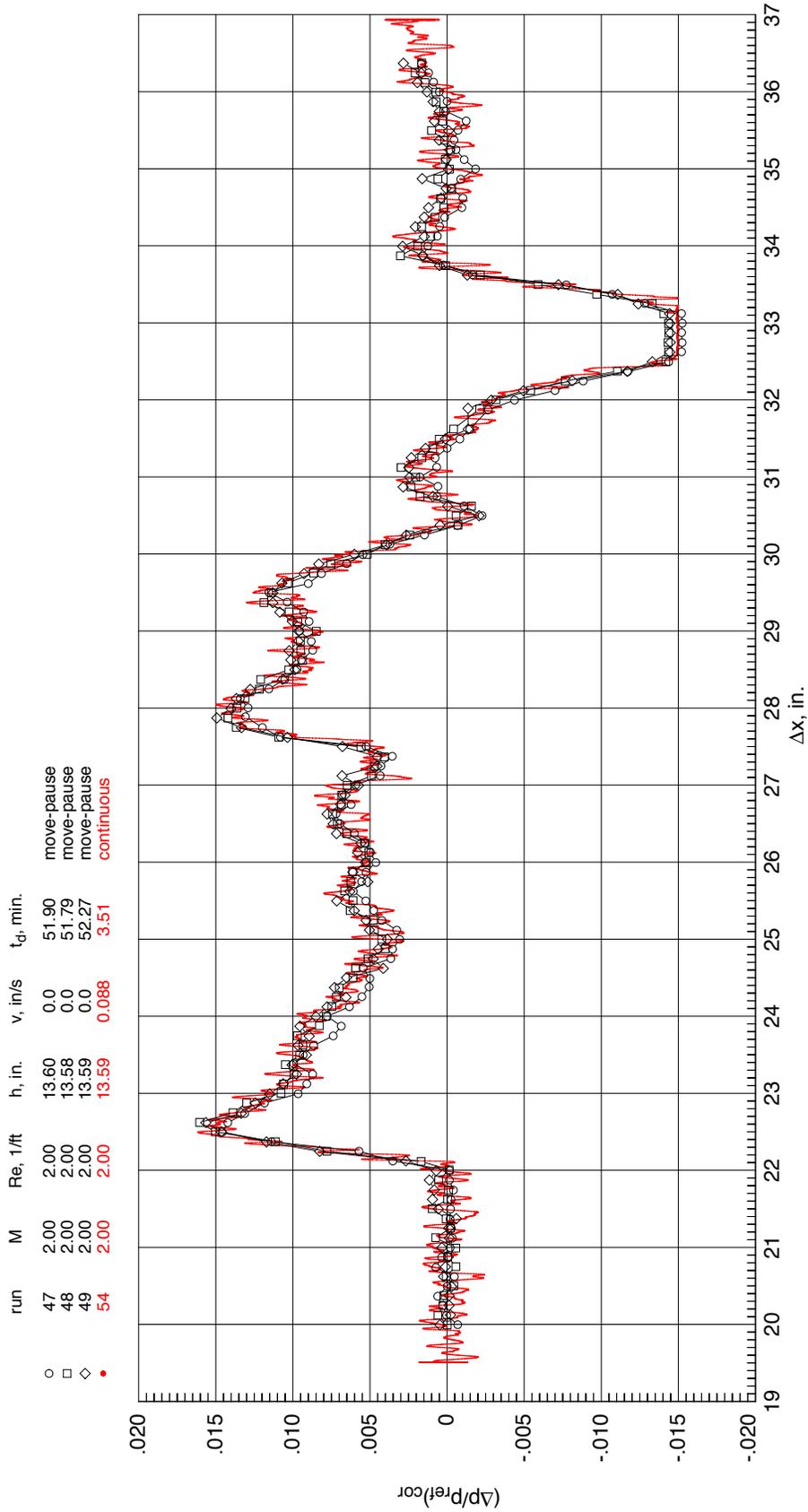
(c) $v = 0.088$ in/s.

Figure 12. Continued.
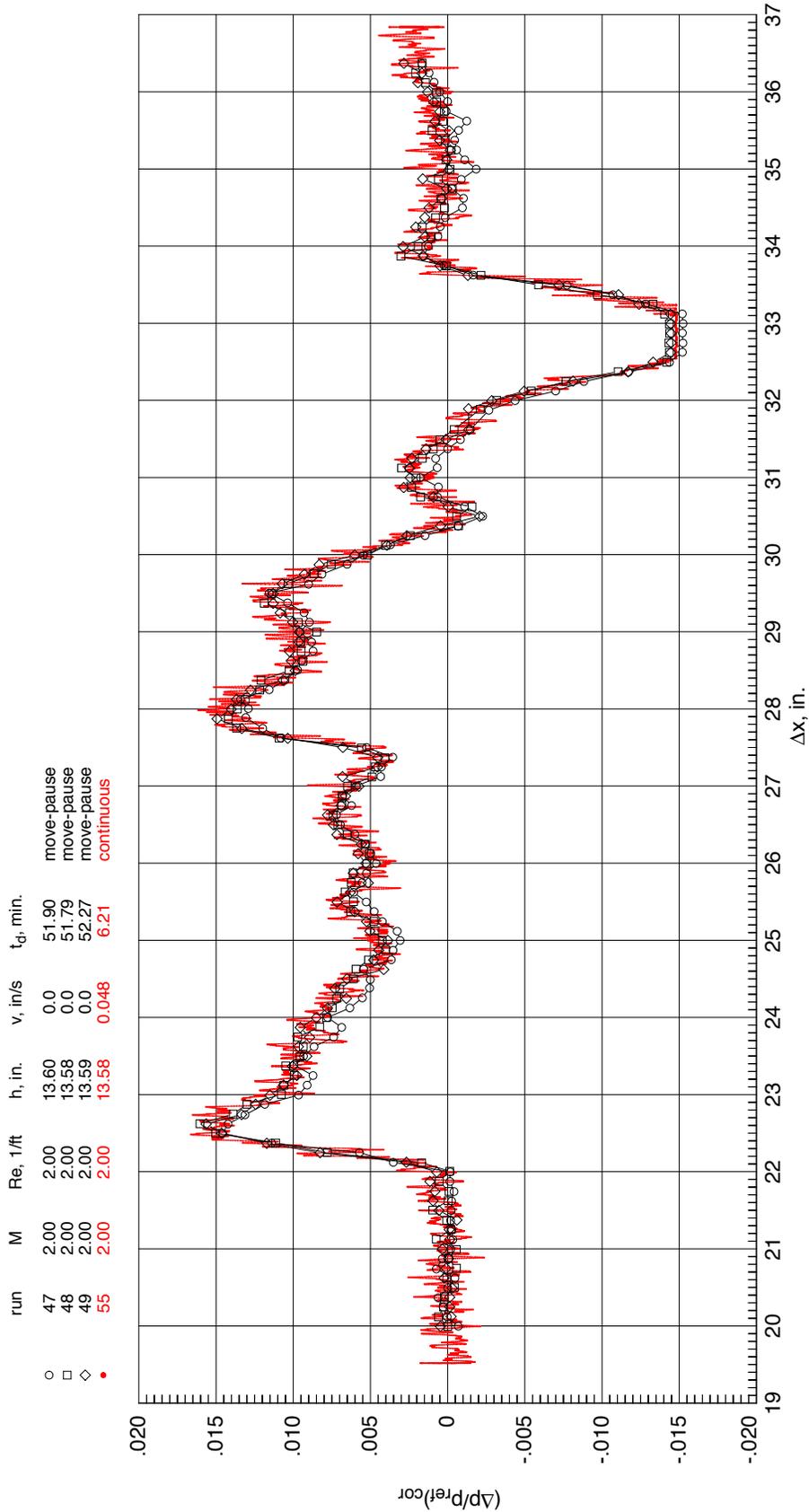
(d) $v = 0.048$ in/s.

Figure 12. Continued.
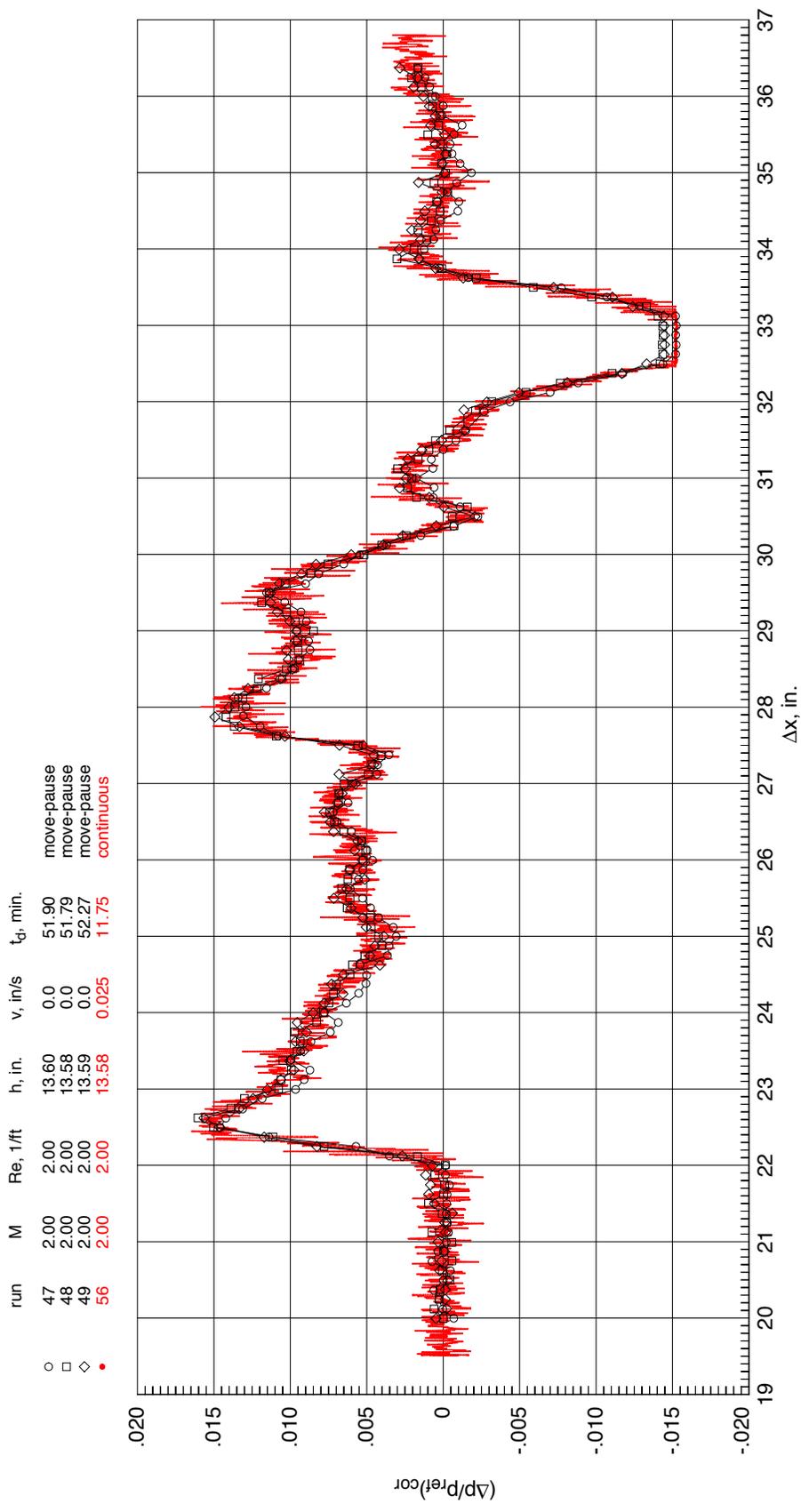
(e) $v = 0.025$ in/s.

Figure 12. Concluded.
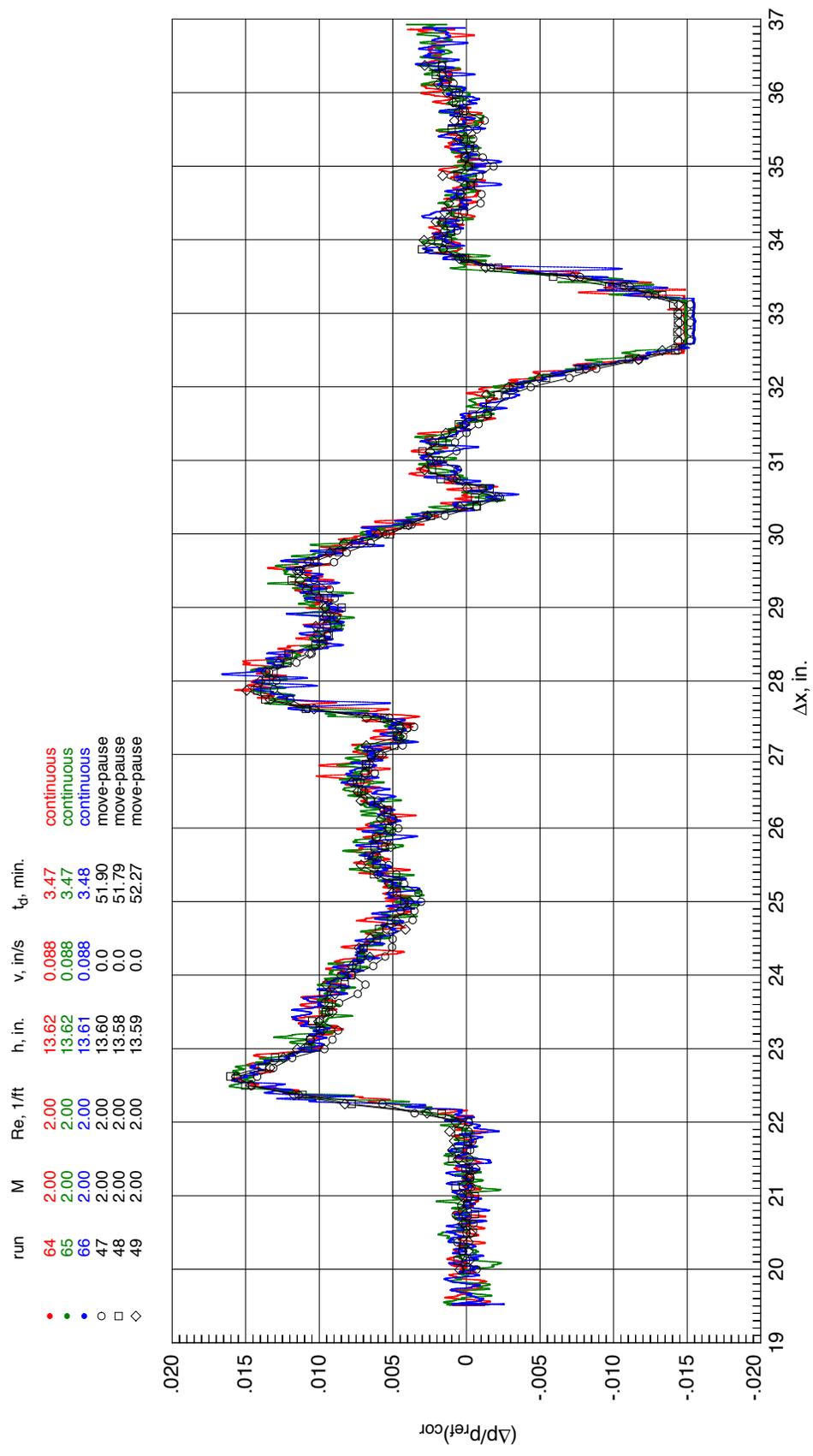
(a) First set of repeats.

Figure 13. Comparison of sonic boom pressure signatures for move-pause and continuous data for each set of back-to-back runs.
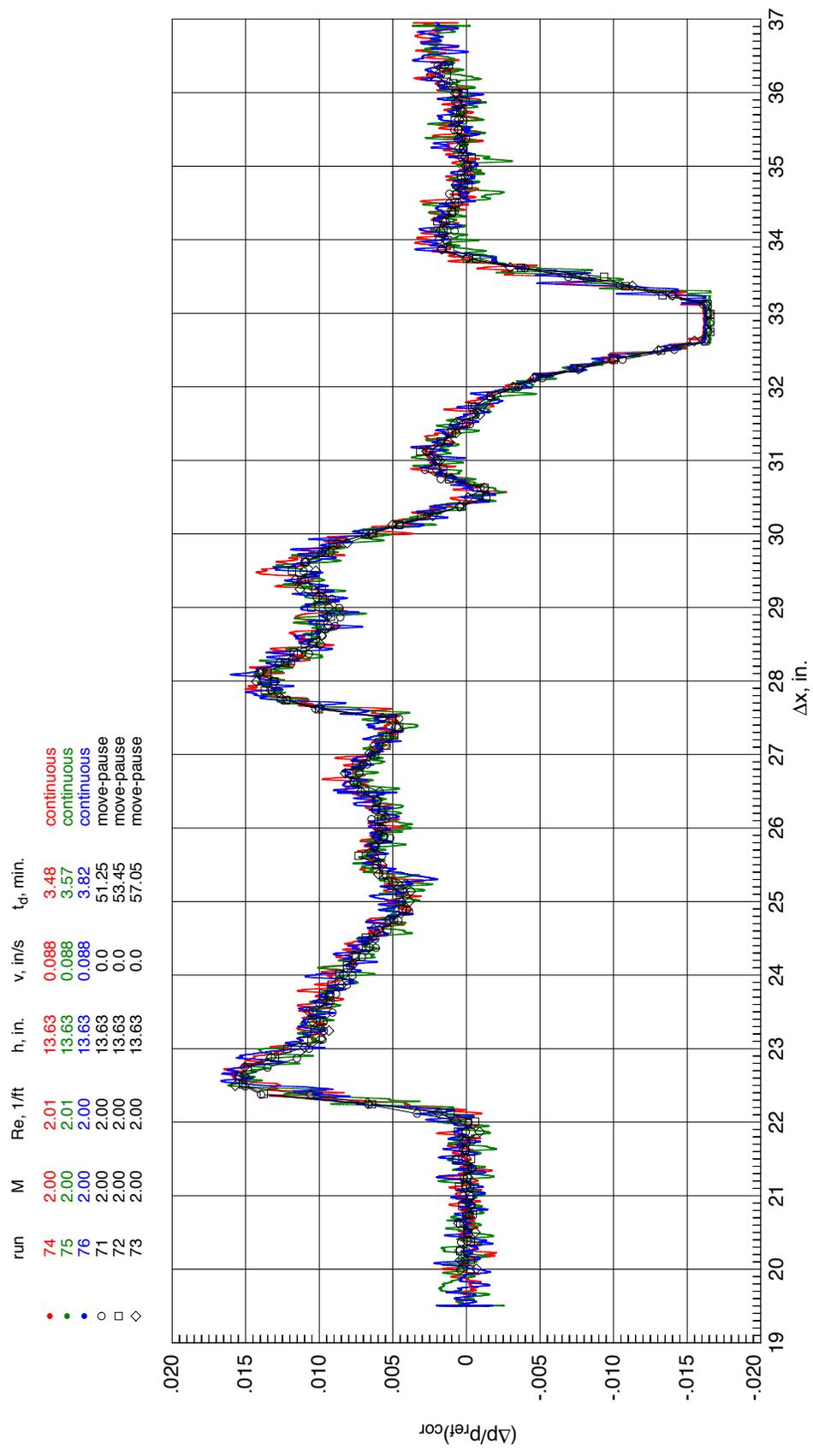
(b) Second set of repeats.

Figure 13. Concluded.
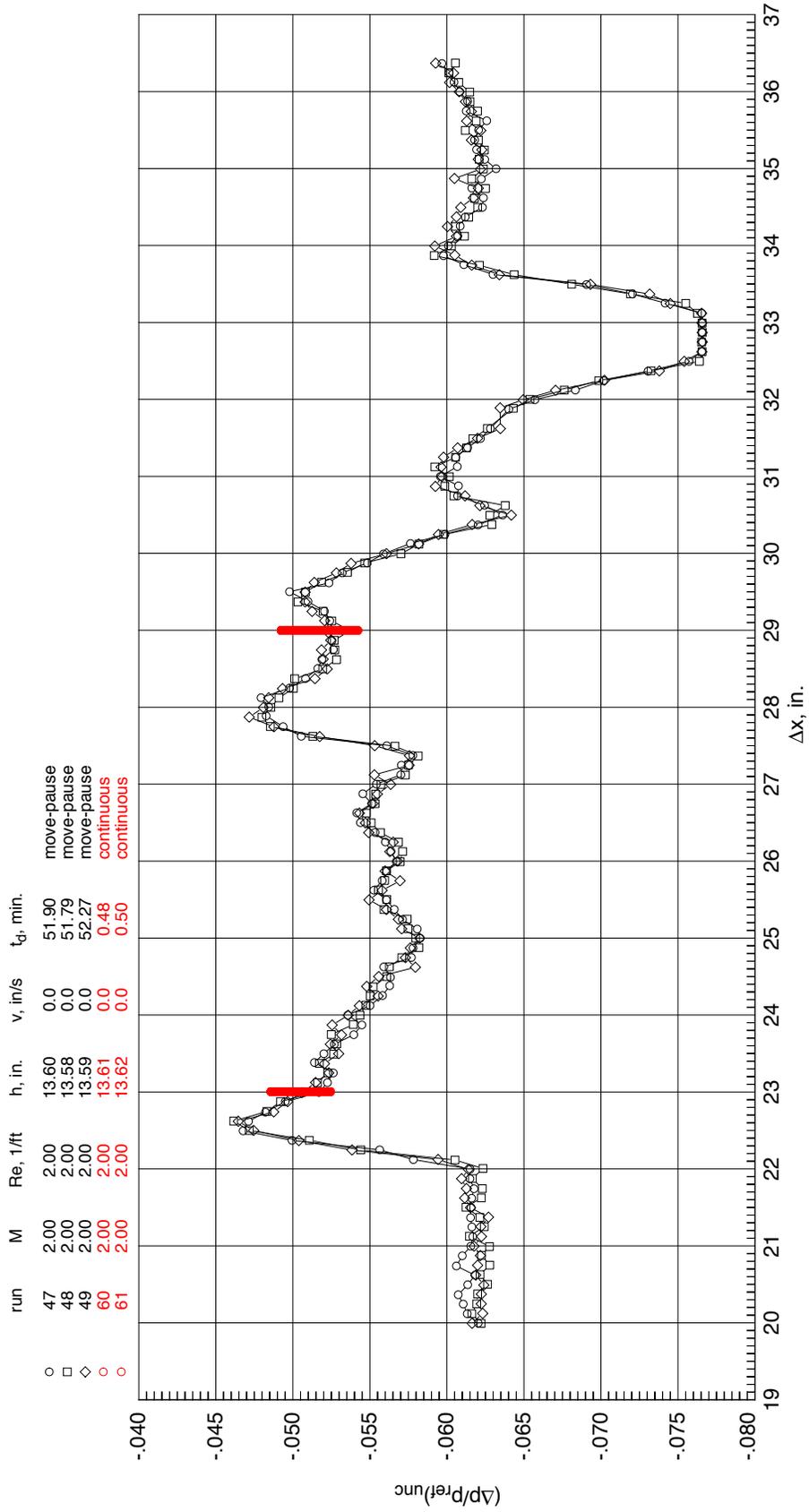
Figure 14. Extent of continuous sonic boom pressure data unsteadiness at two Δx locations compared to move-pause pressure signatures.
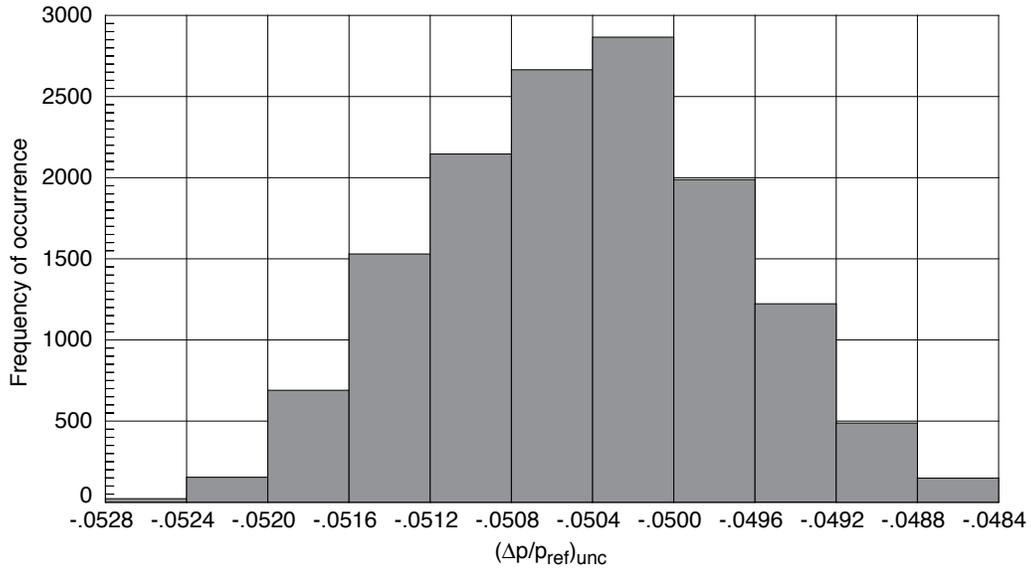
(a) $\Delta x = 23$ in.
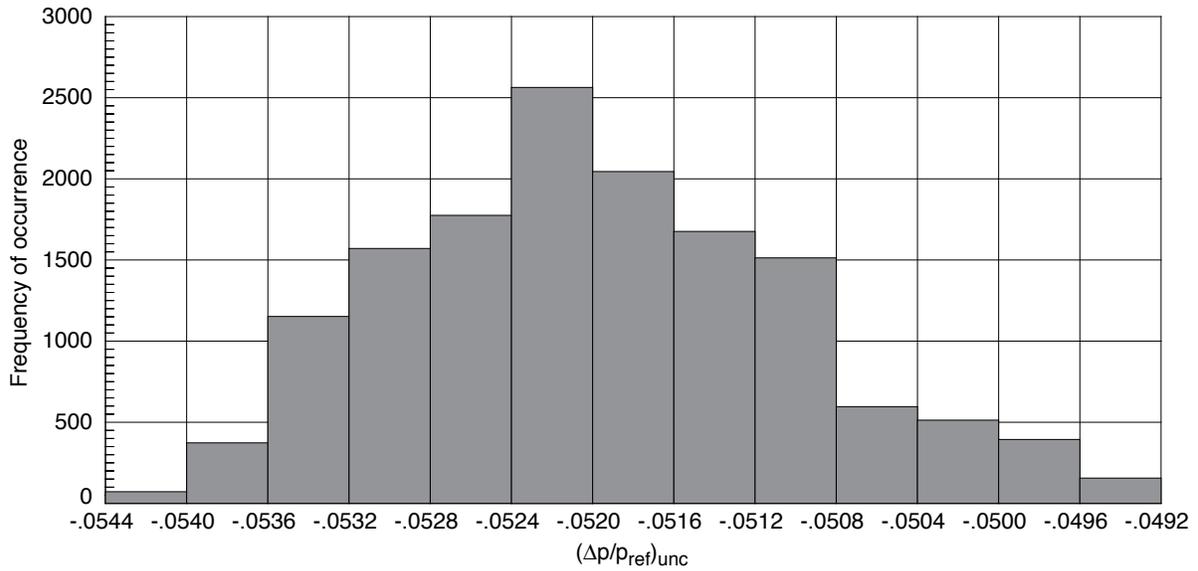
(b) $\Delta x = 29$ in.

Figure 15. Histogram of continuous data (from figure 14) obtained at a single Δx location over approximately 30 s period.
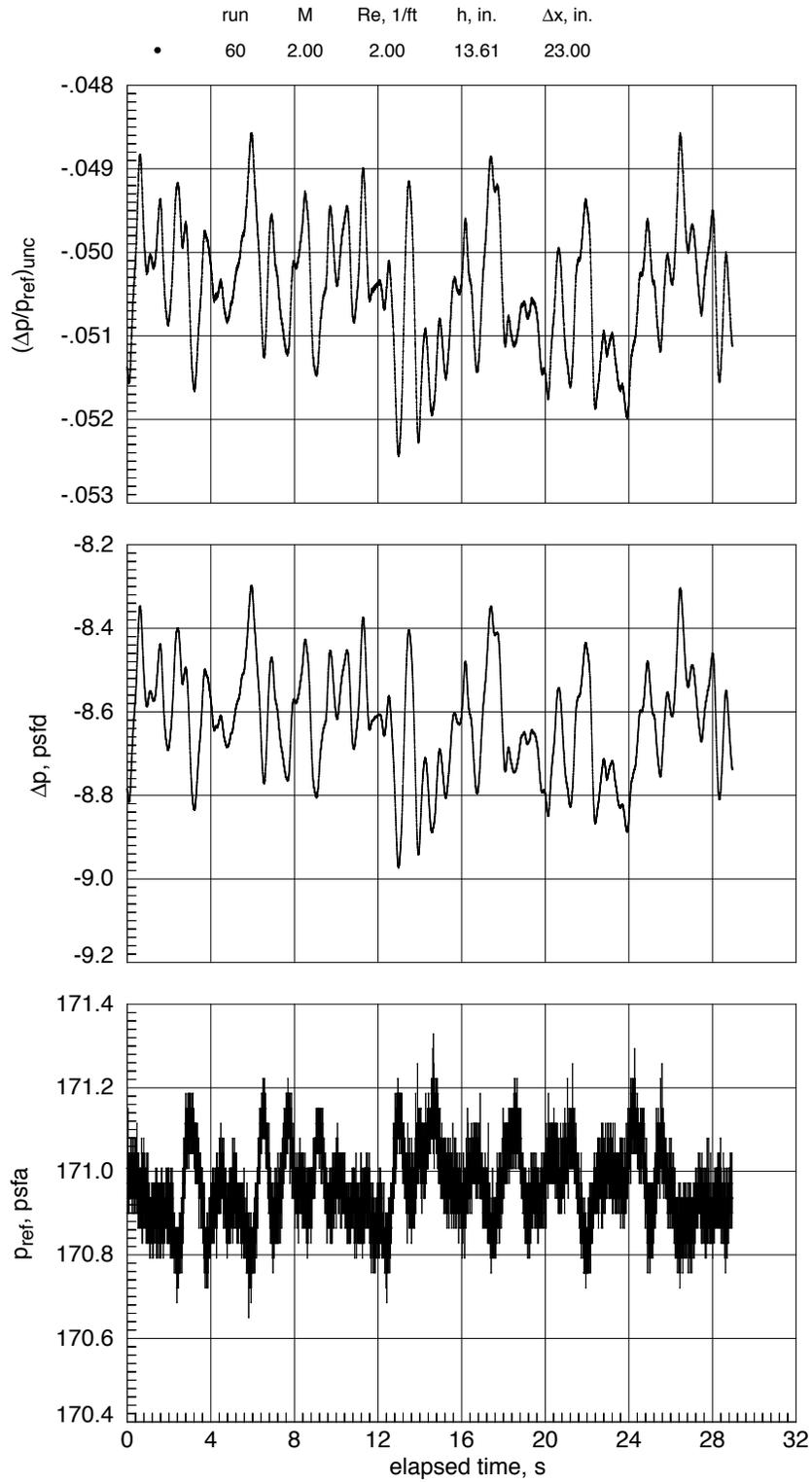
(a) Wind-on.

Figure 16. Differential pressure transducer variation.

39
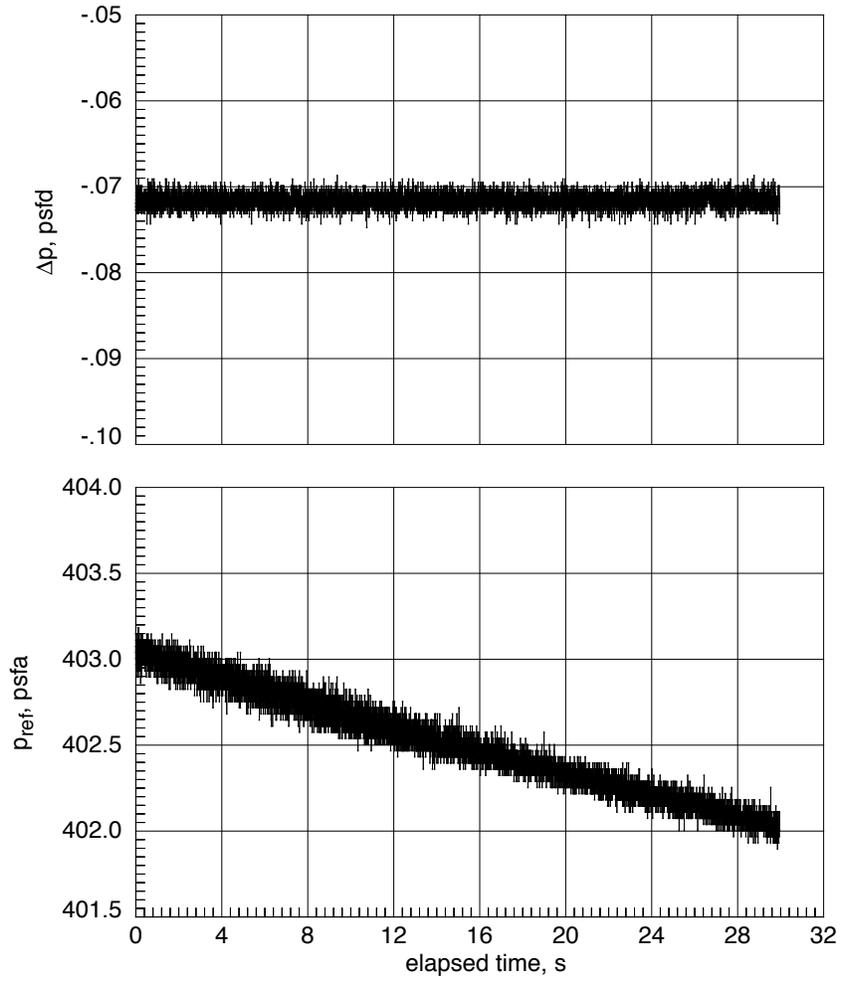
(b) Wind-off.

Figure 16. Concluded.
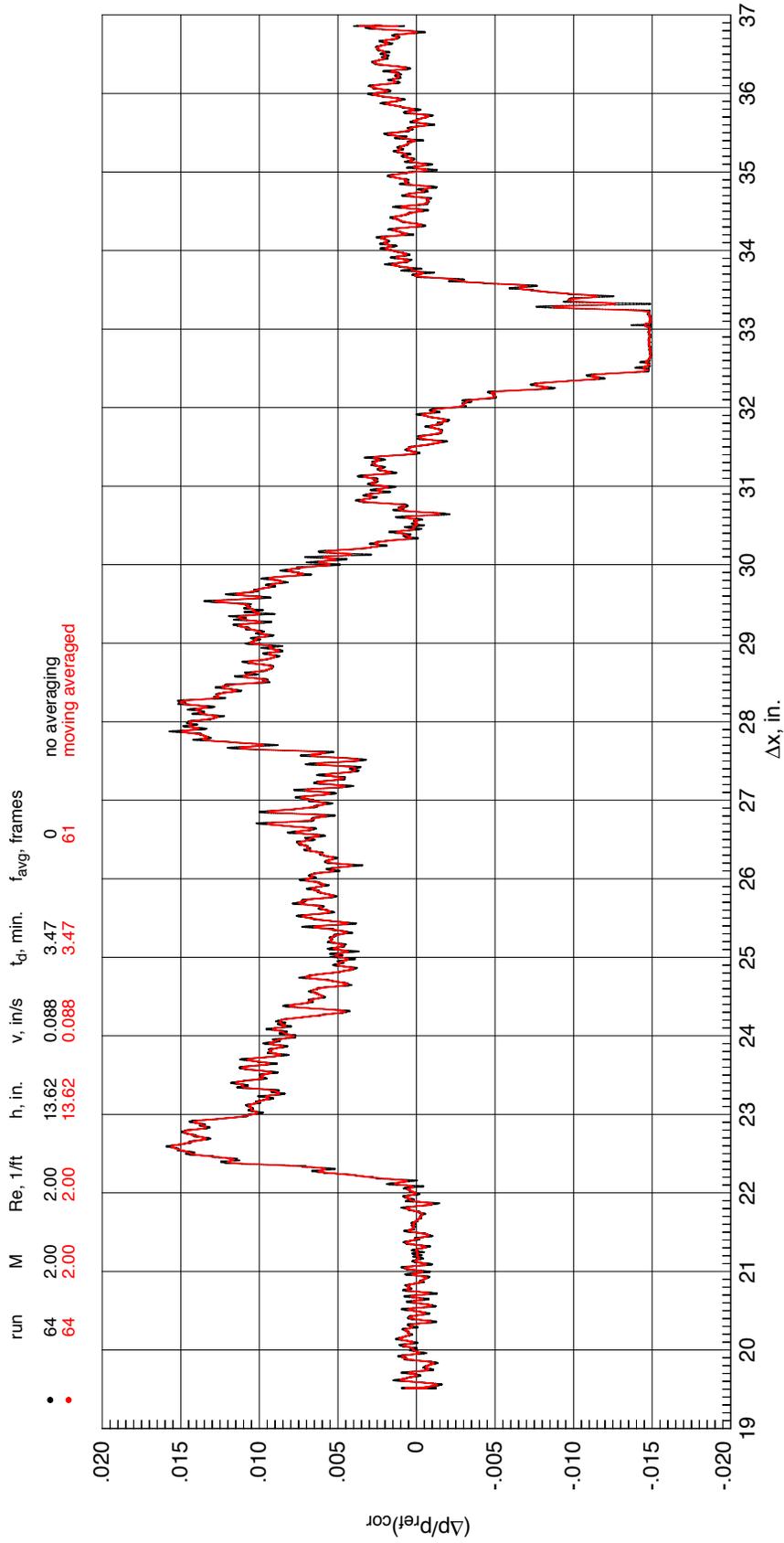
(a) Moving average using 61 frames.

Figure 17. Effect of applying a moving average to continuous sonic boom pressure signature data.
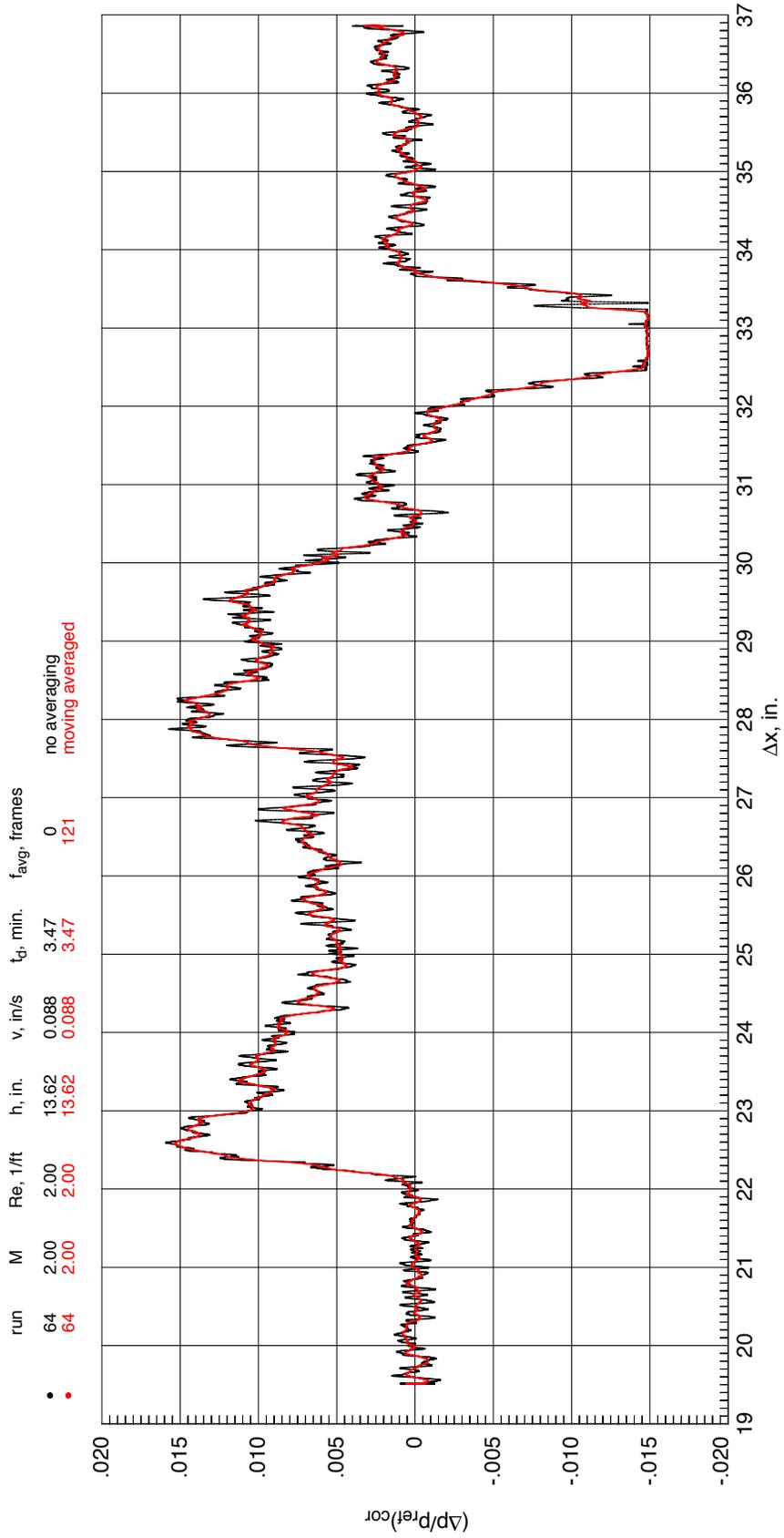
(b) Moving average using 121 frames.

Figure 17. Continued.
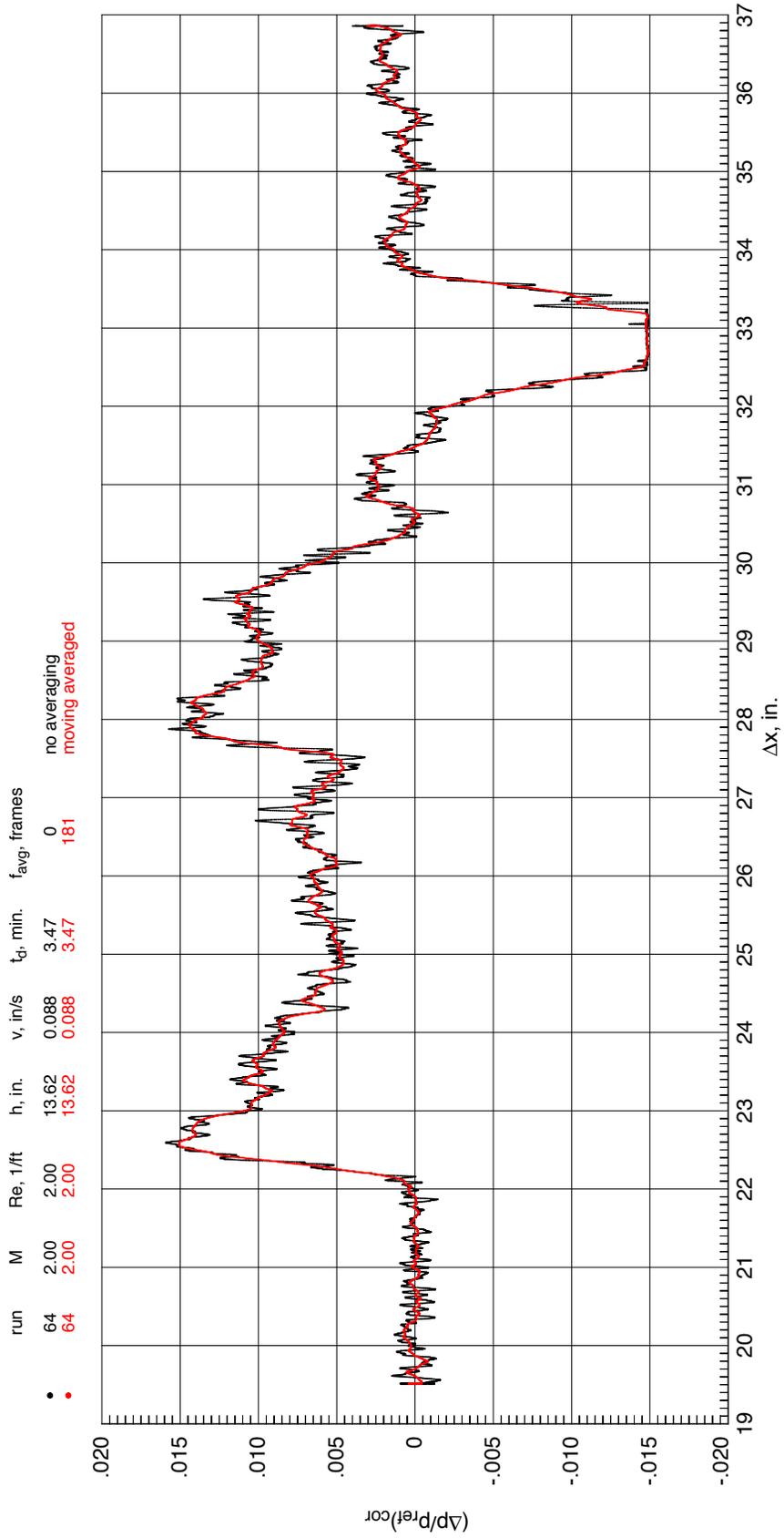
(c) Moving average using 181 frames.

Figure 17. Continued.

43
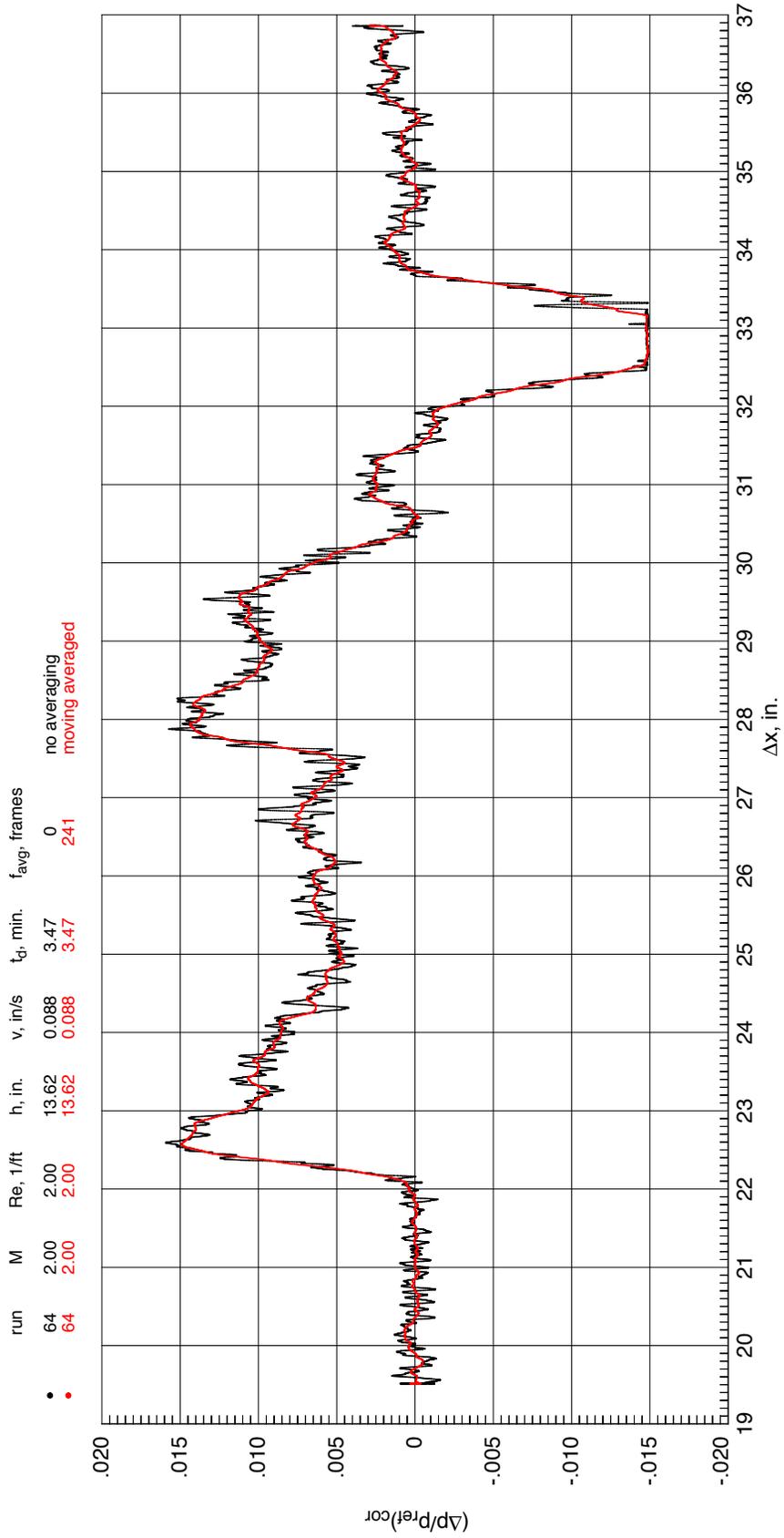
(d) Moving average using 241 frames.

Figure 17. Continued.

44
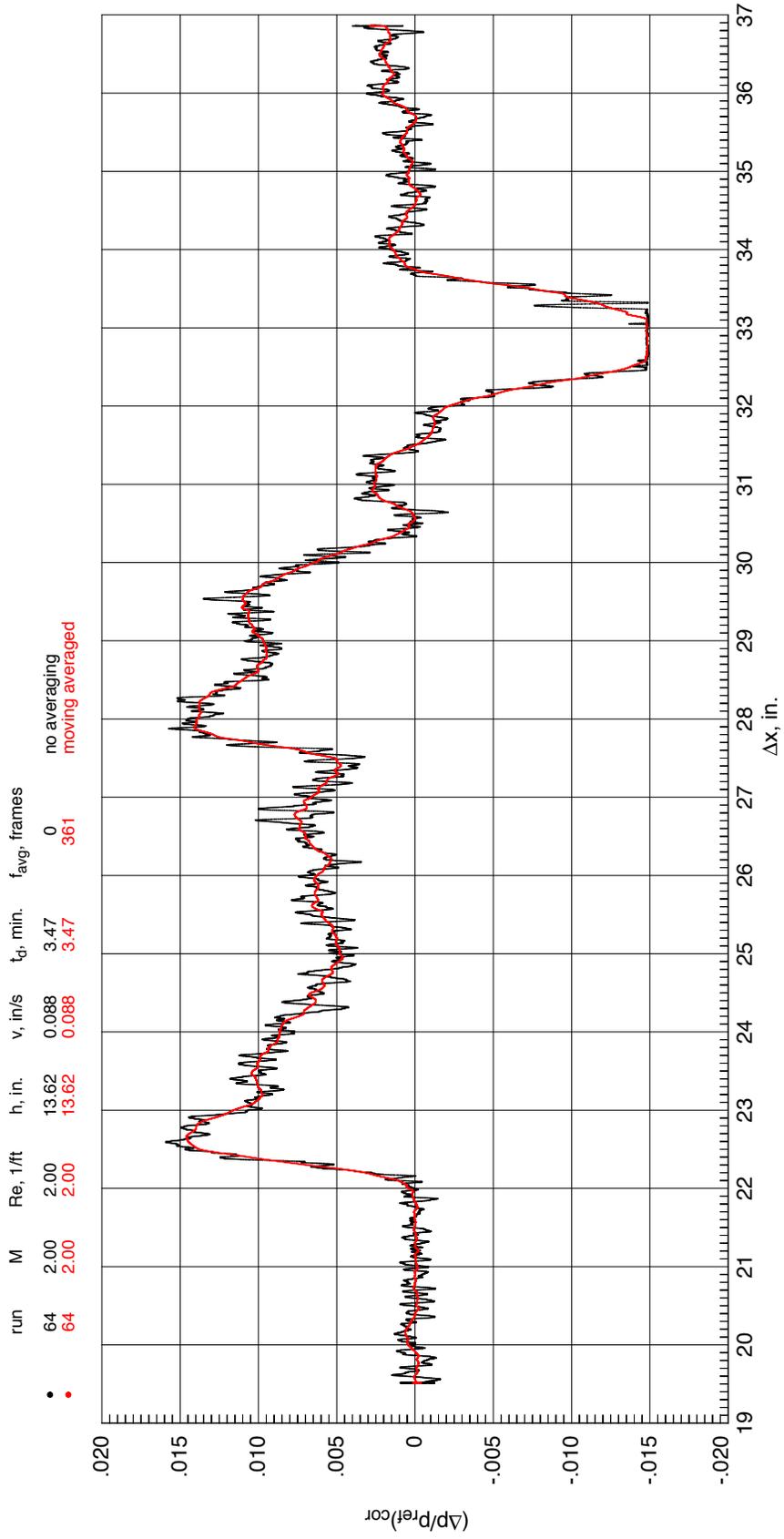
(e) Moving average using 361 frames.

Figure 17. Continued.

45
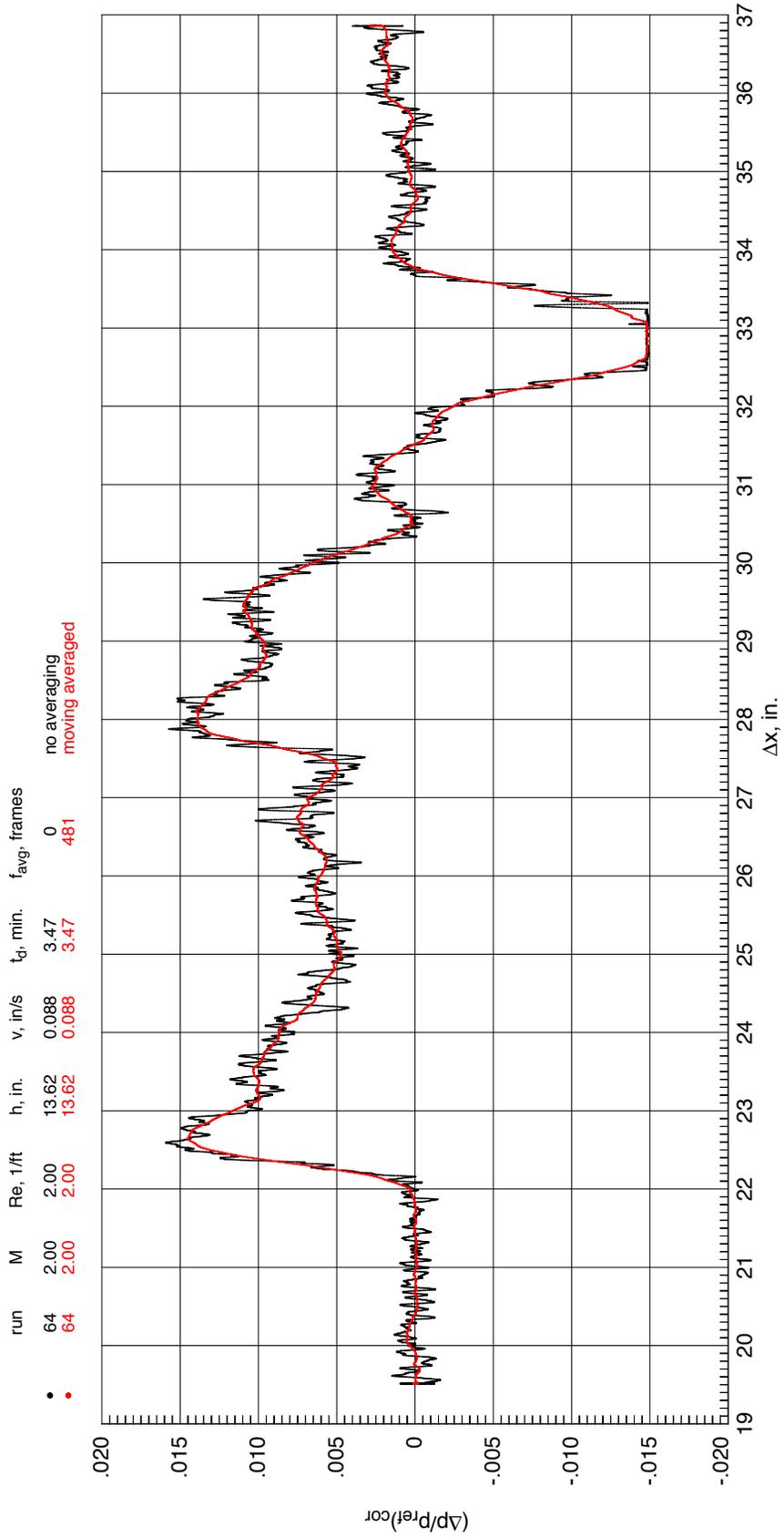
(f) Moving average using 481 frames.

Figure 17. Concluded.
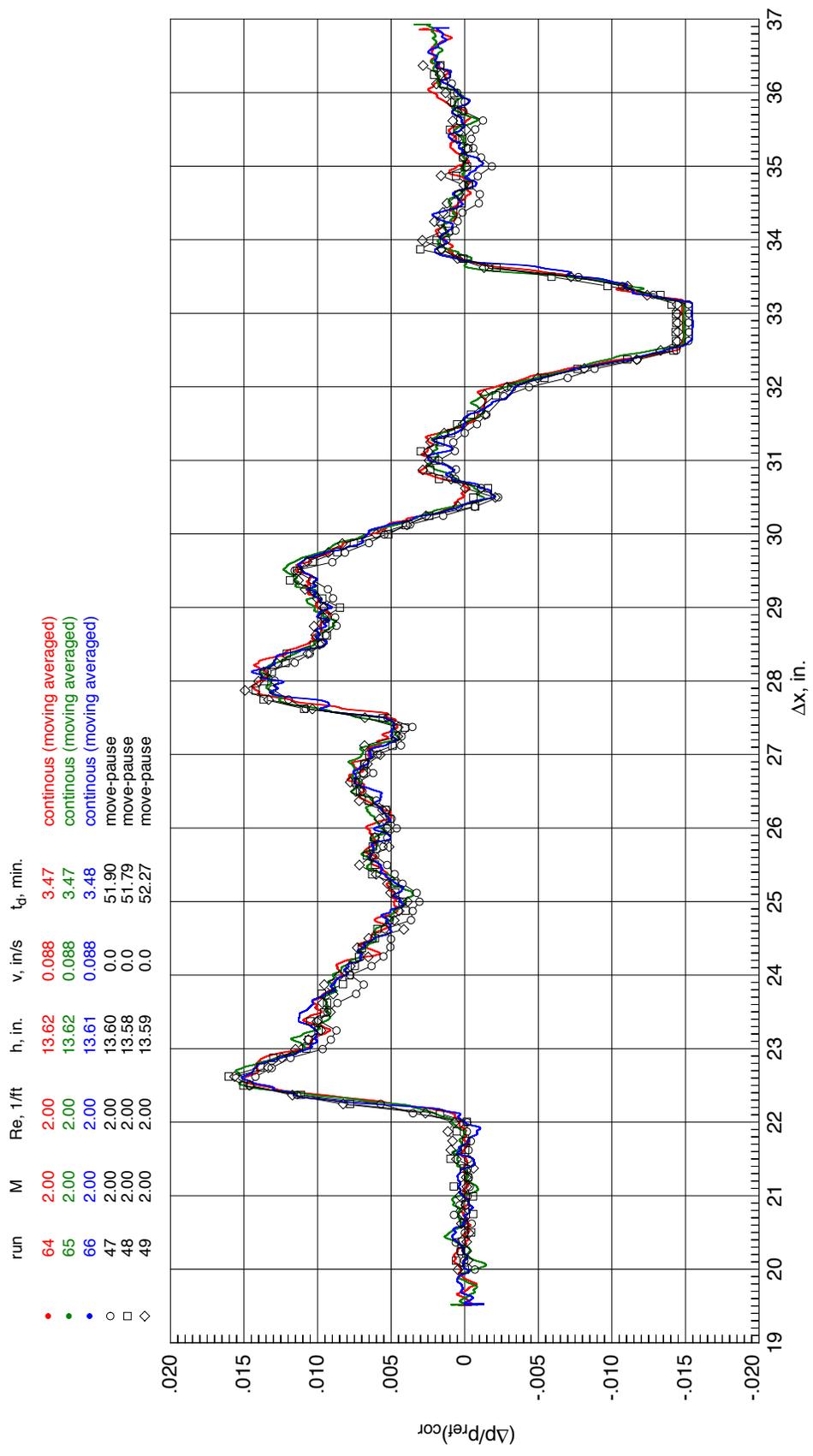
(a) First set of repeats.

Figure 18. Comparison of sonic boom pressure signatures for move-pause and continuous data (moving average applied) for each set of back-to-back runs.
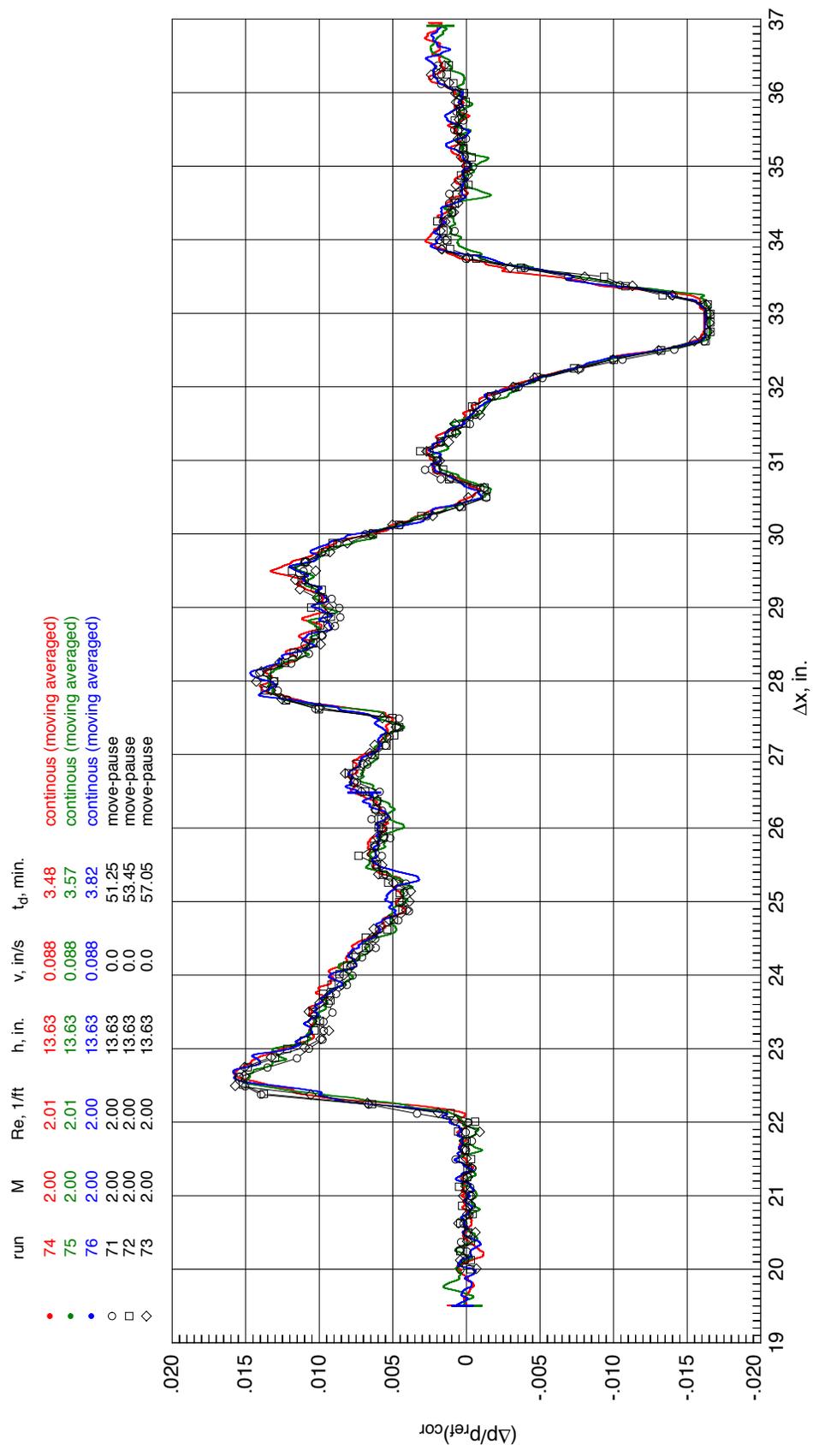
(b) Second set of repeats.

Figure 18. Concluded.

run	M	Re, 1/ft	h, in.	v, in/s	t_d, min.	
47	2.00	2.00	13.60	0.0	51.90	move-pause
48	2.00	2.00	13.58	0.0	51.79	move-pause
49	2.00	2.00	13.59	0.0	52.27	move-pause
71	2.00	2.00	13.63	0.0	51.25	move-pause
72	2.00	2.00	13.63	0.0	53.45	move-pause
73	2.00	2.00	13.63	0.0	57.05	move-pause

● mean of 6 runs with 95 % confidence interval bars

Δx, in.

$(\Delta p/p_{ref})_{cor}$
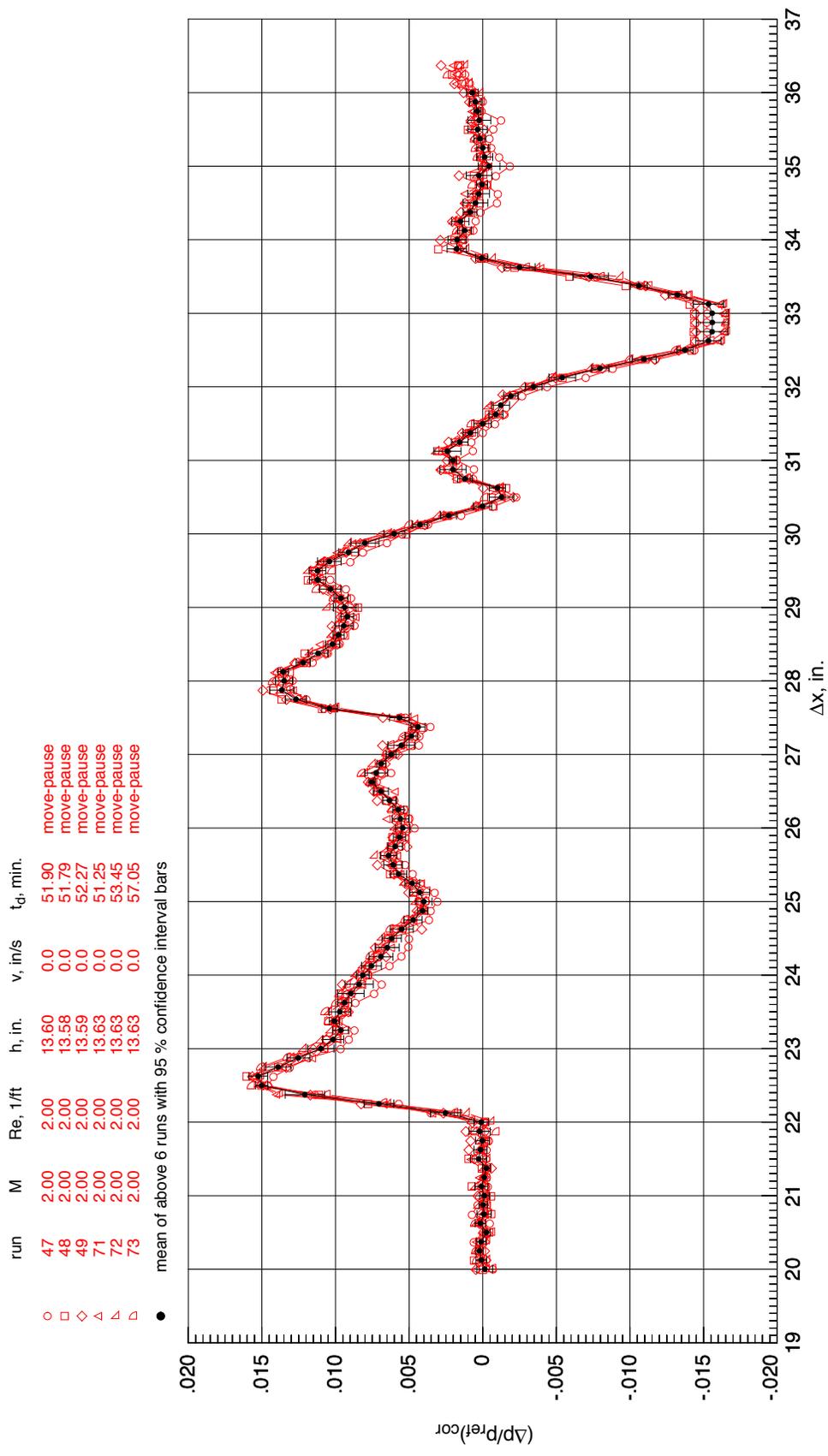
(a) Confidence interval.

Figure 19. Move-pause sonic boom pressure signature data with confidence and prediction intervals at a 95 % significance level.
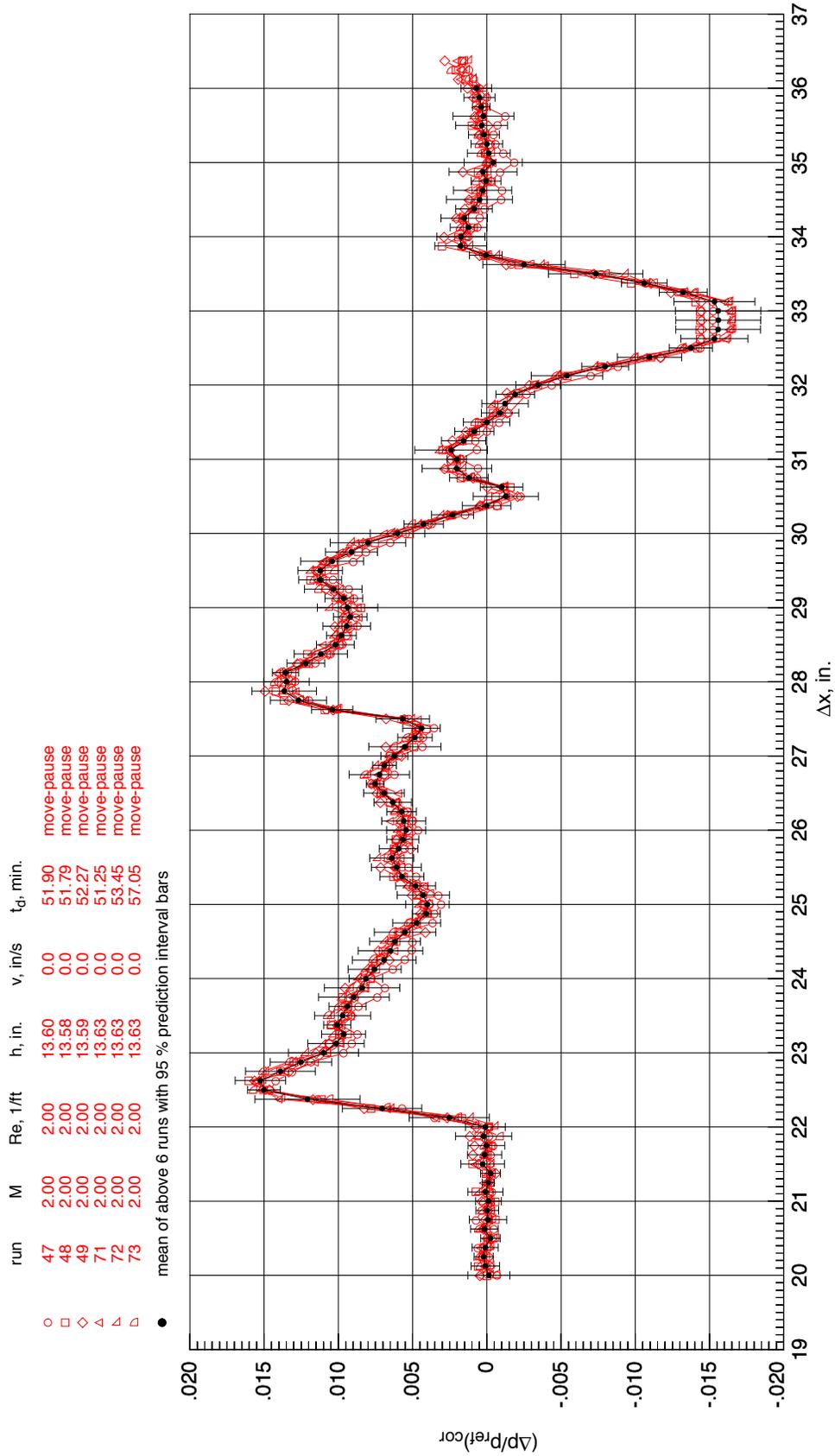
(b) Prediction interval.

Figure 19. Concluded.

Figure 20. Continuous sonic boom pressure signature data (no moving average applied) at specific Δx locations with confidence and prediction intervals at a 95 % significance level.

(a) Confidence interval.
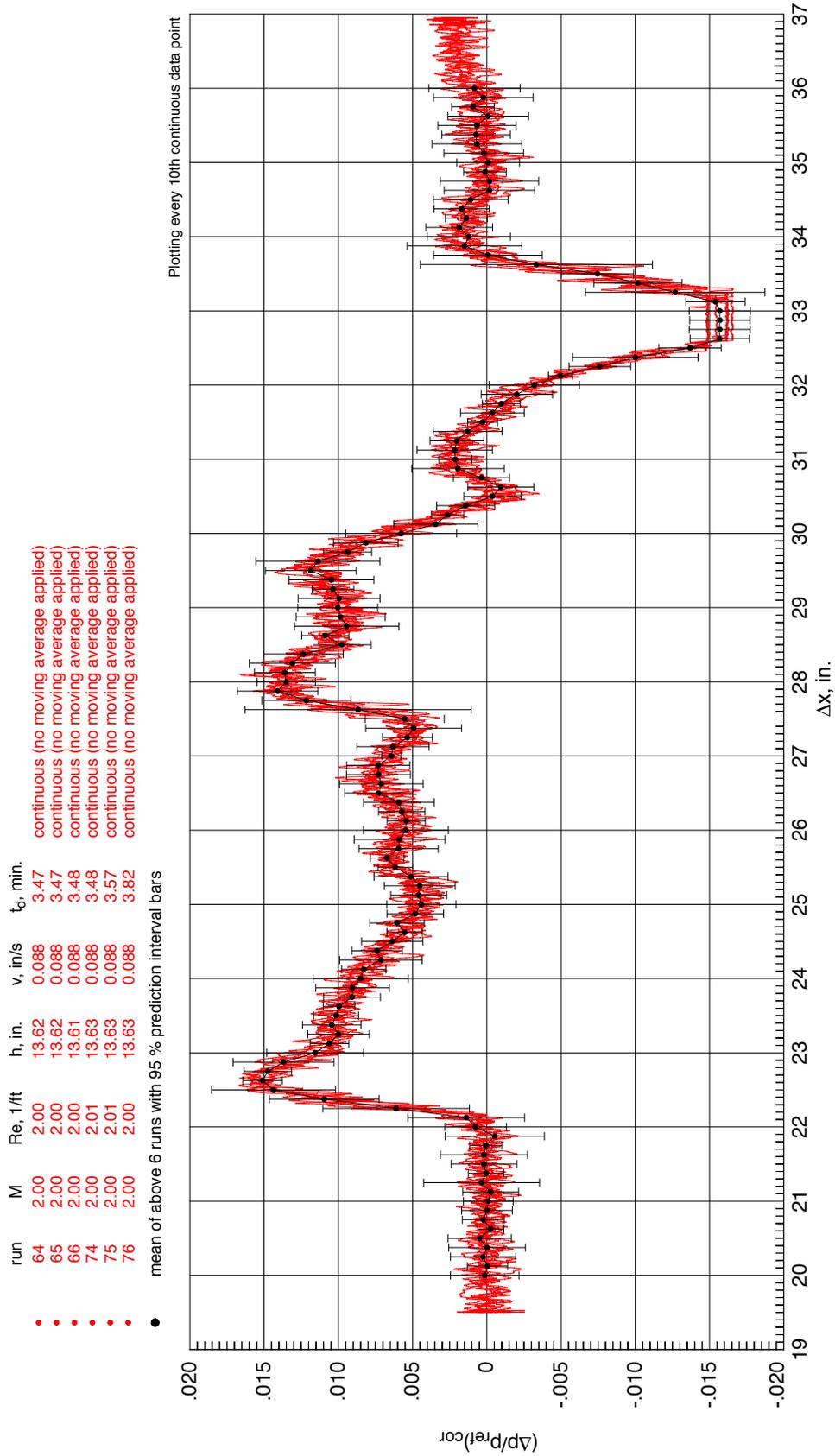
(b) Prediction interval.

Figure 20. Concluded.

Figure 21. All six continuous data runs (moving average applied) and mean values at specific Δx locations with confidence and prediction intervals at a 95 % level.

(a) Confidence interval.
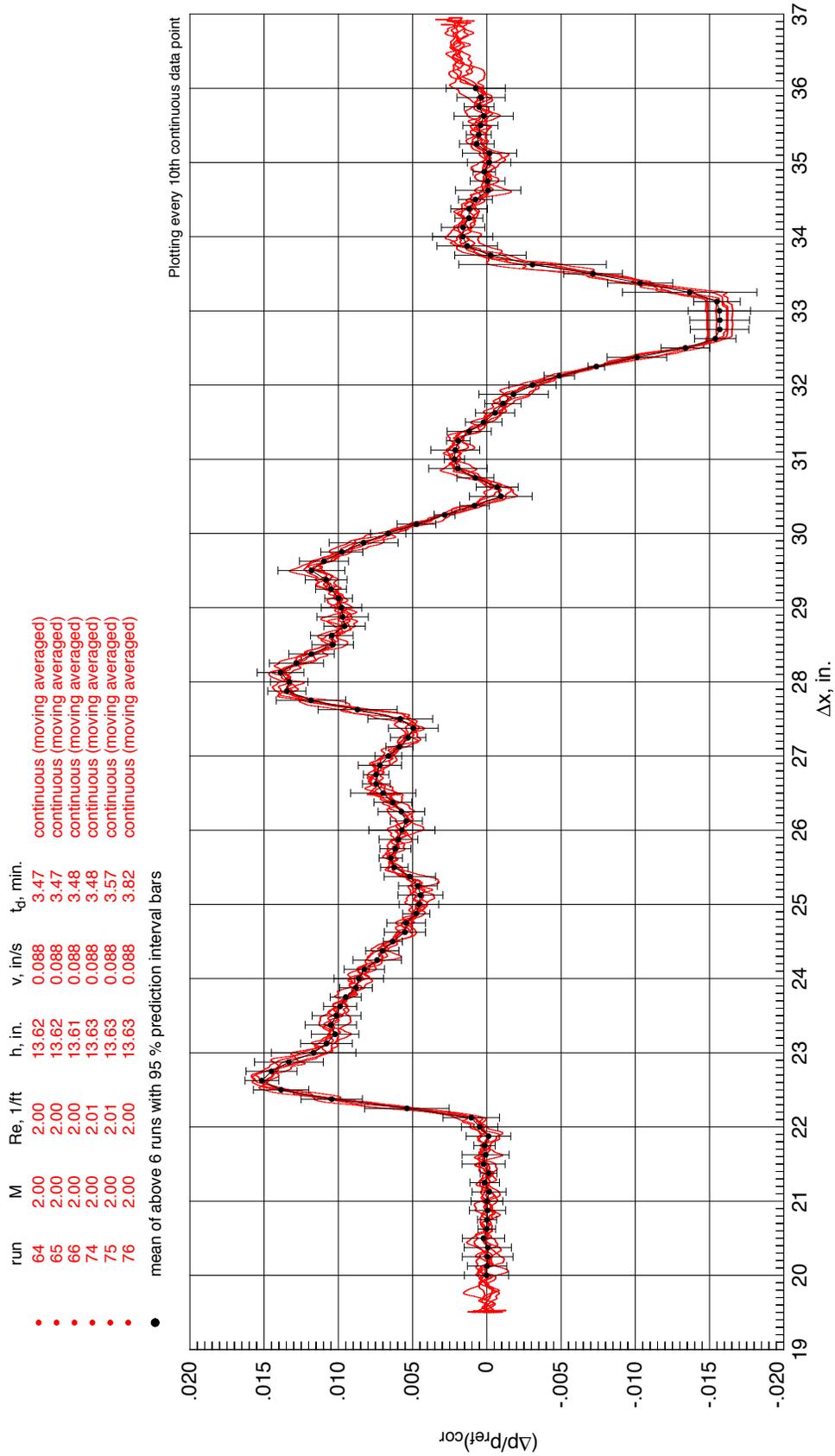
(b) Prediction interval.

Figure 21. Concluded.

54
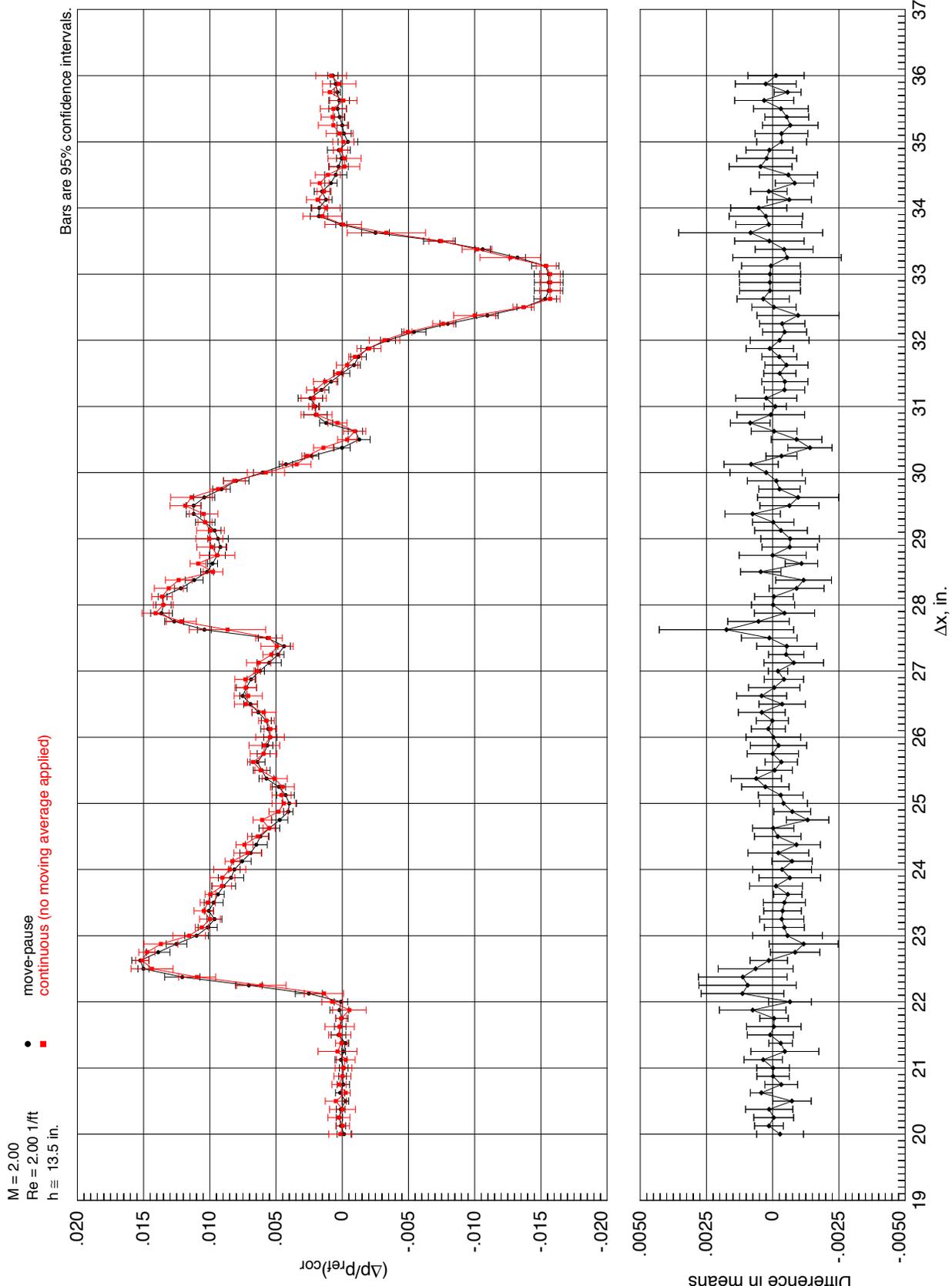
(a) No moving average applied to continuous data.

Figure 22. Comparison of mean values of move-pause and continuous data along with the difference in means with confidence intervals at a 95 % significance level.
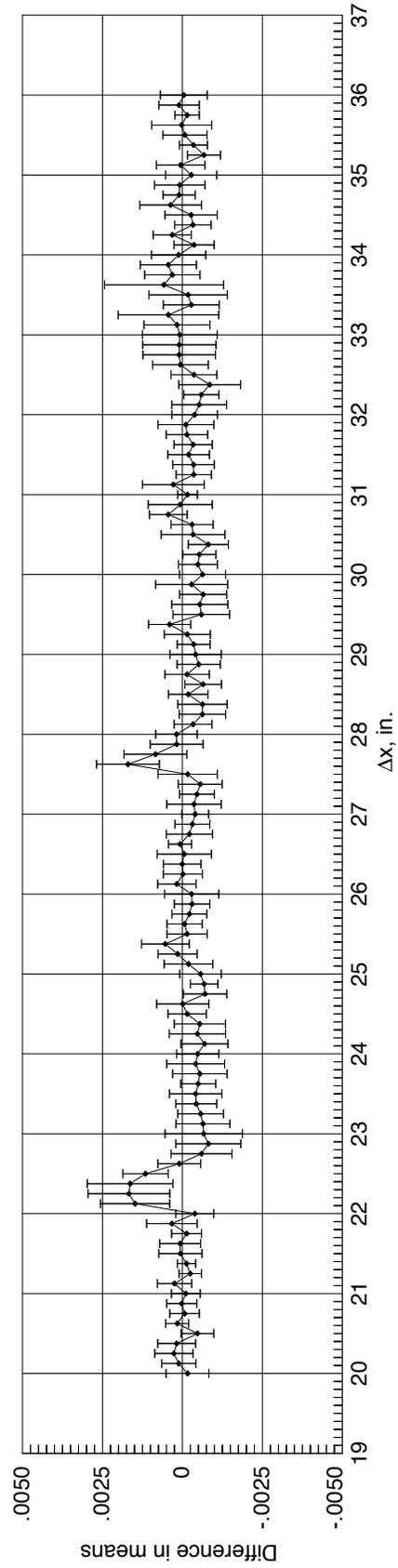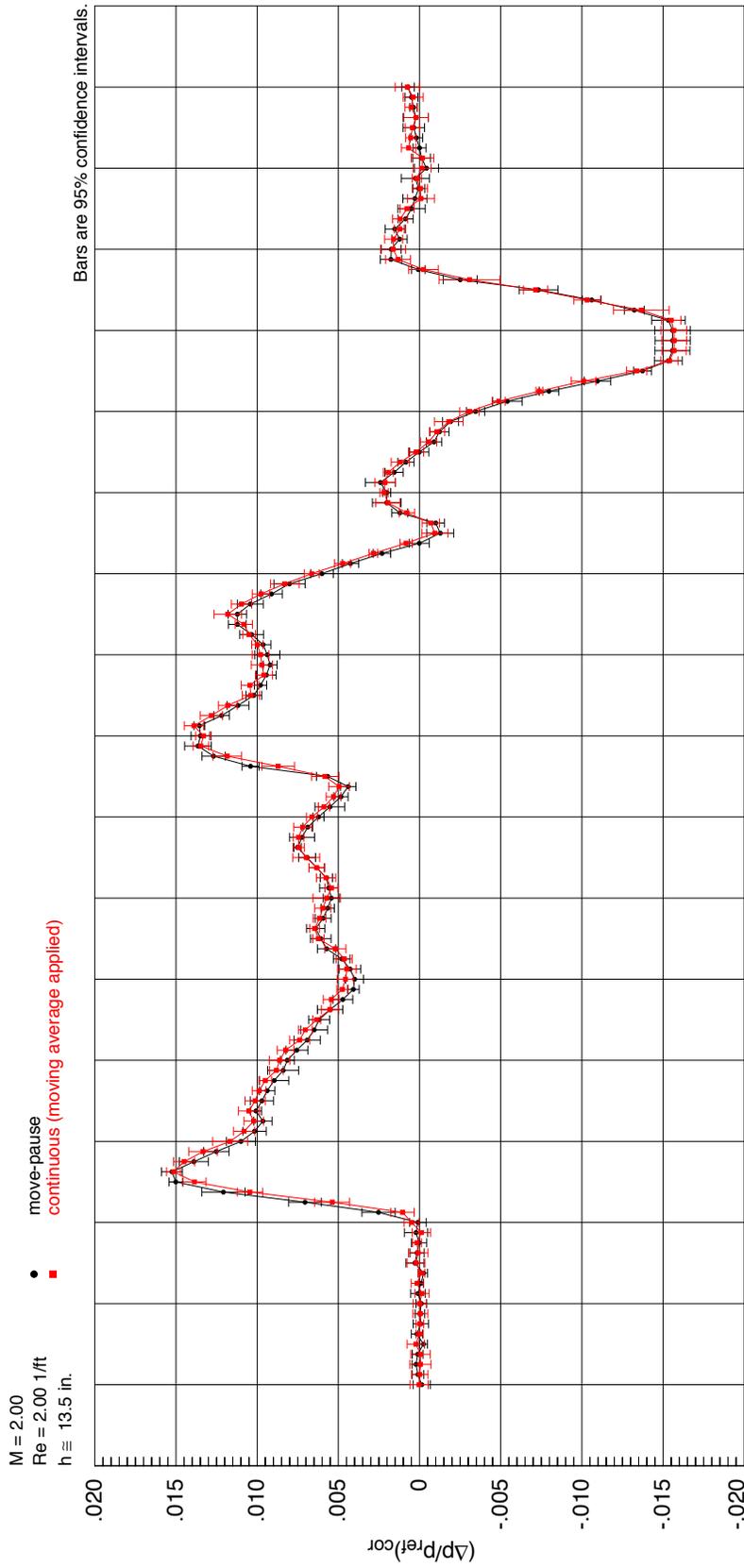
(b) Moving average applied to continuous data.

Figure 22. Concluded.

56
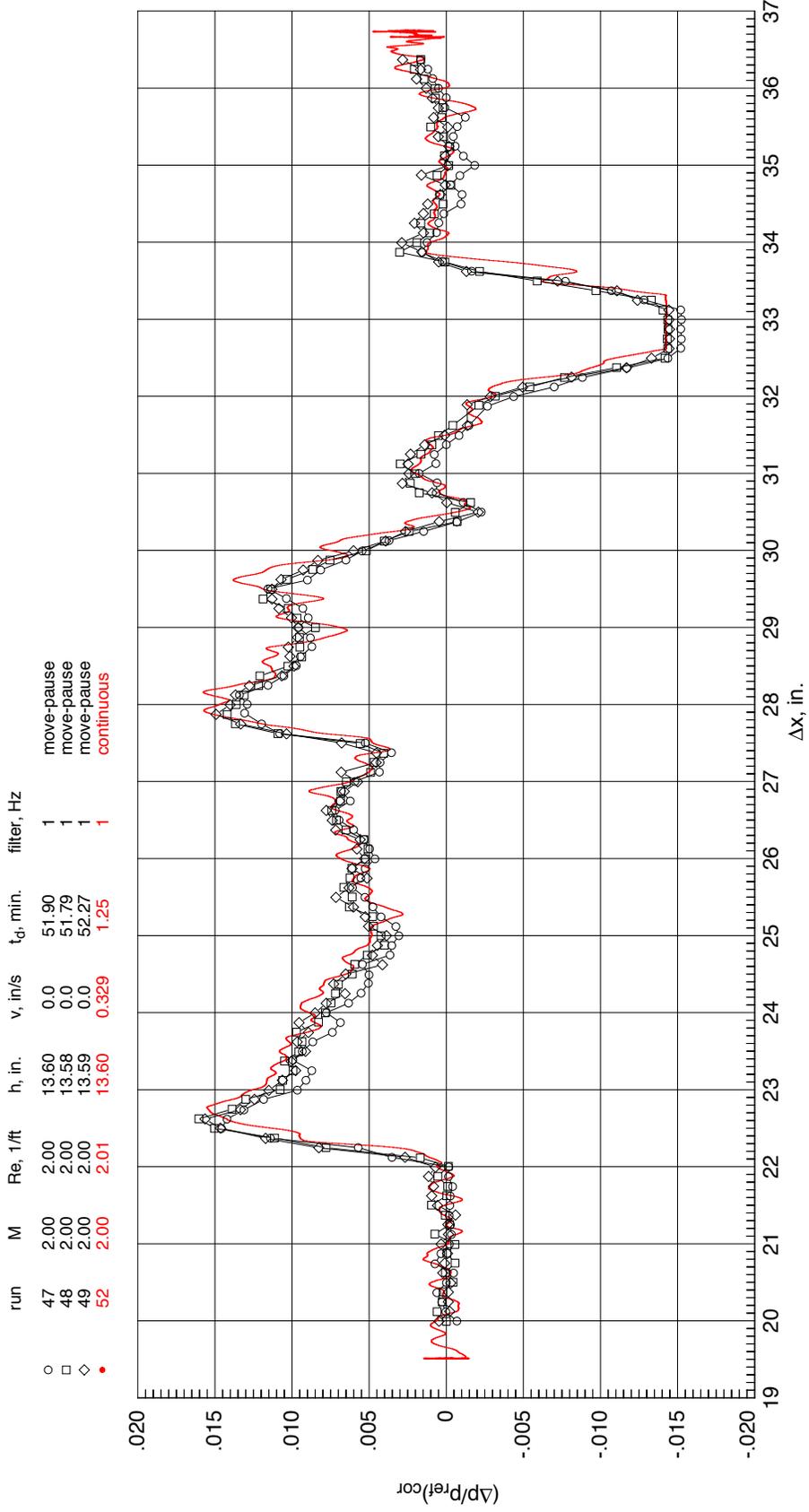
(a) 1 Hz low-pass filter.

Figure 23. Comparison of sonic boom pressure signatures for move-pause and continuous data obtained at various data acquisition system filter settings.
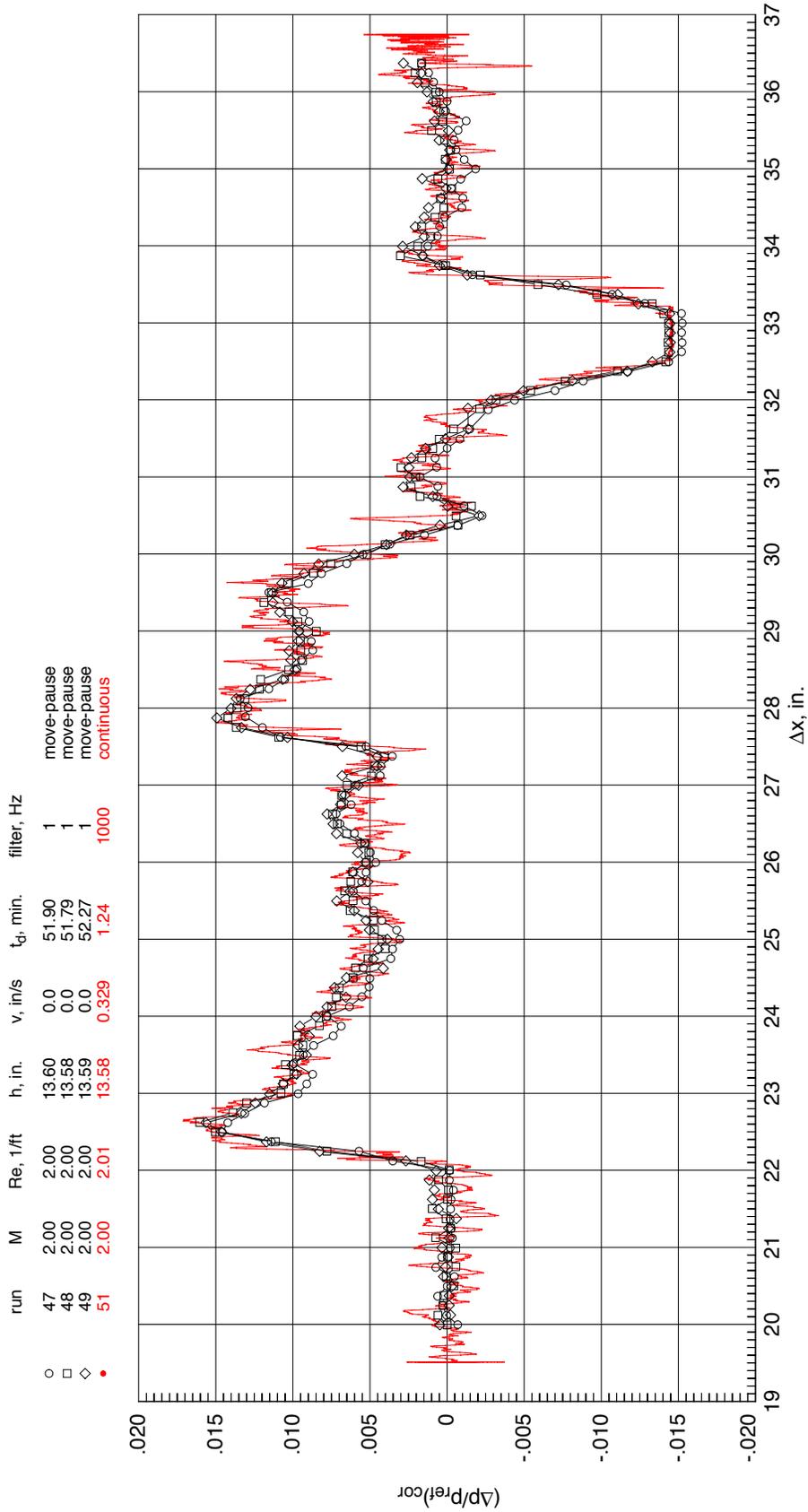
(b) 1000 Hz low-pass filter.

Figure 23. Concluded.

Appendix

Equations for Calculation of Confidence and Prediction Intervals

The equations used to compute the confidence intervals for the mean of the six move-pause runs and six continuous data runs were obtained from reference 17. The symbols used in the equations presented below are defined in this appendix.

The sample mean was computed from:

$$\text{sample mean} = \bar{x} = \frac{\sum\limits_{i=1}^{n} x_i}{n}$$

where,
x_i = individual sample
n = number of samples

The sample standard deviation that is used in the calculation of the confidence and prediction intervals was computed from:

$$\text{sample standard deviation} = s = \sqrt{\frac{\sum\limits_{i=1}^{n} x_i^2 - \dfrac{\left(\sum\limits_{i=1}^{n} x_i\right)^2}{n}}{n-1}}$$

The confidence interval on the mean for the move-pause and continuous data runs was computed from:

$$\text{confidence interval} = \bar{x} \pm (t_{\alpha/2, n-1}) \frac{s}{\sqrt{n}}$$

where,
$t_{\alpha/2, n-1}$ = two-tailed t distribution value at a $100(1 - \alpha)$ % confidence level for $n - 1$ degrees of freedom
α = level of significance (0.05 used in this paper)

Finally, the prediction interval on the mean for the move-pause and continuous data runs was computed from:

$$\text{prediction interval} = \bar{x} \pm (t_{\alpha/2, n-1}) s \sqrt{1 + \frac{1}{n}}$$

The equations used to compute the confidence intervals for the difference in means between the move-pause and continuous data runs were obtained from reference 17 and are shown below:

$$\text{pooled standard deviation} = s_p = \sqrt{\frac{(n_1 - 1)s_1^2 + (n_2 - 1)s_2^2}{n_1 + n_2 - 1}}$$

where,
n_1 = number of samples from sample set 1
n_2 = number of samples from sample set 2
s_1 = sample standard deviation from sample set 1
s_2 = sample standard deviation from sample set 2

$$\text{confidence interval on difference in means} = (\bar{x}_1 - \bar{x}_2) \pm (t_{\alpha/2, n_1+n_2-2}) s_p \sqrt{\frac{1}{n_1} + \frac{1}{n_2}}$$

where,
$t_{\alpha/2, n_1+n_2-2}$ = two-tailed t distribution value at a $100(1-\alpha)$ % significance level for
$\qquad n_1 + n_2 - 2$ degrees of freedom
$\bar{x}_1$ = mean from sample set 1
$\bar{x}_2$ = mean from sample set 2

REPORT DOCUMENTATION PAGE

1. REPORT DATE (DD-MM-YYYY)	2. REPORT TYPE	3. DATES COVERED (From – To)
01–08–2013	Technical Publication	

4. TITLE AND SUBTITLE

Experimental Measurement of Sonic Boom Signatures Using a Continuous Data Acquisition Technique

5a. CONTRACT NUMBER

5b. GRANT NUMBER

5c. PROGRAM ELEMENT NUMBER

6. AUTHOR(S)

Wilcox, Floyd J., Jr.; Elmiligui, Alaa A.

5d. PROJECT NUMBER

5e. TASK NUMBER

5f. WORK UNIT NUMBER

122711.03.07.07.16.80

7. PERFORMING ORGANIZATION NAME(S) AND ADDRESS(ES)

NASA Langley Research Center
Hampton, VA 23681–2199

8. PERFORMING ORGANIZATION REPORT NUMBER

L-20226

9. SPONSORING/MONITORING AGENCY NAME(S) AND ADDRESS(ES)

National Aeronautics and Space Administration
Washington, DC 20546–0001

10. SPONSOR/MONITOR'S ACRONYM(S)

NASA

11. SPONSOR/MONITOR'S REPORT NUMBER(S)

NASA/TP–2013–218035

12. DISTRIBUTION/AVAILABILITY STATEMENT

Unclassified - Unlimited
Subject Category 02
Availability: NASA CASI (443) 757-5802

13. SUPPLEMENTARY NOTES

14. ABSTRACT

A wind tunnel investigation was conducted in the Langley Unitary Plan Wind Tunnel to determine the effectiveness of a technique to measure aircraft sonic boom signatures using a single conical survey probe while continuously moving the model past the probe. Sonic boom signatures were obtained using both move-pause and continuous data acquisition methods for comparison. The test was conducted using a generic business jet model at a constant angle of attack and a single model-to-survey-probe separation distance. The sonic boom signatures were obtained at a Mach number of 2.0 and a unit Reynolds number of 2 million per foot. The test results showed that it is possible to obtain sonic boom signatures while continuously moving the model and that the time required to acquire the signature is at least 10 times faster than the move-pause method. Data plots are presented with a discussion of the results. No tabulated data or flow visualization photographs are included.

15. SUBJECT TERMS

Sonic boom; Aerodynamics; Supersonics; Wind tunnel test; Continuous data acquisition; Sonic boom pressure signature

16. SECURITY CLASSIFICATION OF:			17. LIMITATION OF ABSTRACT	18. NUMBER OF PAGES	19a. NAME OF RESPONSIBLE PERSON
a. REPORT	b. ABSTRACT	c. THIS PAGE			STI Help Desk (email: help@sti.nasa.gov)
U	U	U	UU	65	**19b. TELEPHONE NUMBER** (Include area code) (443) 757-5802